UNIVERSIDADE FEDERAL DO RIO DE JANEIRO

INSTITUTO DE FÍSICA

Optimized charging processes for quantum batteries

Yohan Vianna de Almeida

Tese de Doutorado apresentada ao Programa de Pós-Graduação em Física do Instituto de Física da Universidade Federal do Rio de Janeiro - UFRJ, como parte dos requisitos necessários à obtenção do título de Doutor em Ciências (Física).

Orientador: Marcelo P. E. F. Santos

Rio de Janeiro

Abril de 2025

OPTIMIZED CHARGING PROCESSES FOR QUANTUM BATTERIES

Yohan Vianna de Almeida

Orientador: Marcelo P. E. F. Santos.

Tese de Doutorado submetida ao Programa de Pós-Graduação em Física do Instituto de Física da Universidade Federal do Rio de Janeiro - UFRJ, como parte dos requisitos necessários à obtenção do título de Doutor em Ciências (Física).

Aprovada por:

Prof. Dr. Marcelo P. E. F. Santos - IF/UFRJ

(Presidente e orientador)

Prof. Dr. Ruynet Lima de Matos Filho - IF/UFRJ

Prof. Dr. Gabriel Horacio Aguilar - IF/UFRJ

Profa. Dra. Nadja Kolb Bernardes - UFPE

Prof. Dr. Felipe Javier Barra de la Guarda - UCHILE

Rio de Janeiro, RJ - Brasil

Abril de 2025

CIP - Catalogação na Publicação

V447o

Vianna de Almeida, Yohan
Optimized charging processes for quantum batteries / Yohan Vianna de Almeida. -- Rio de Janeiro, 2025.
102 f.

Orientador: Marcelo Paleólogo Elefteriadis de França Santos.
Tese (doutorado) - Universidade Federal do Rio de Janeiro, Instituto de Física, Programa de Pós Graduação em Física, 2025.

1. baterias quânticas. 2. termodinâmica quântica. 3. ótica quântica. 4. sistemas abertos. 5. mecânica quântica. I. Paleólogo Elefteriadis de França Santos, Marcelo, orient. II. Título.

Elaborado pelo Sistema de Geração Automática da UFRJ com os dados fornecidos pelo(a) autor(a), sob a responsabilidade de Miguel Romeu Amorim Neto - CRB-7/6283.

Resumo

Optimized charging processes for quantum batteries

Yohan Vianna de Almeida

Orientador: Marcelo P. E. F. Santos

Resumo da tese de Doutorado apresentada ao Programa de Pós-Graduação em Física do Instituto de Física da Universidade Federal do Rio de Janeiro - UFRJ, como parte dos requisitos necessários à obtenção do título de Doutor em Ciências (Física).

Desde suas primeiras formulações, no início do século XX, a teoria quântica tem revolucionado diversas áreas do conhecimento humano e sustenta praticamente todas as tecnologias utilizadas no mundo moderno. Medicina, química, comunicações são só alguns exemplos das várias áreas que receberam positivos impactos advindos da capacidade de entender, prever e manipular o mundo microscópico. Ao findar do século XX e início do novo milênio, o desenvolvimento tecnológico da época tornou possível manipular novos conceitos que foram fundamentais para o entendimento de fenômenos verdadeiramente quânticos. Assim, termos como *superposição* e *emaranhamento* ganharam destaque no mundo científico e a busca pelo desenvolvimento de novas tecnologias que aplicam efeitos quânticos intrínsecos ao mundo microscópico foi impulsionada. Desenvolvimento de detectores mais sensíveis, aplicações em redes de comunicação e armazenamento de energia foram alguns dos novos alvos durante a chamada *segunda revolução quântica*, que se estende até os dias de hoje. Nesta tese, desenvolvem-se métodos de otimização de carregamento para as chamadas *baterias quânticas*, que são sistemas microscópicos fabricados com o intuito de armazenar energia para ser usada posteriormente em alguma tarefa

de interesse. Utilizamos o paradigma dos sistemas quânticos abertos, que é a descrição fornecida para sistemas microscópicos que sofrem com efeitos deletérios do meio no qual estão inseridos. Aqui, desenvolvemos algumas maneiras de aproveitar recursos quânticos presentes no sistema (como coerências quânticas, por exemplo) para otimizar o processo de carregamento das baterias.

Palavras-chave: bateria quântica; sistemas quânticos abertos; tecnologias quânticas; qubit; cavidades ressonantes; termodinâmica quântica; calibre; simetrias; QED; ótica quântica.

Abstract

Optimized charging processes for quantum batteries

Yohan Vianna de Almeida

Orientador: Marcelo P. E. F. Santos

Abstract da tese de Doutorado apresentada ao Programa de Pós-Graduação em Física do Instituto de Física da Universidade Federal do Rio de Janeiro - UFRJ, como parte dos requisitos necessários à obtenção do título de Doutor em Ciências (Física).

Since its first formulations, in the beginning of the 20th century, the quantum theory has revolutionized different areas of the human knowledge and supports practically all the technologies present in the modern world. Medicine, chemistry, communications are only a few examples from various fields that received positive impacts arising from the ability to comprehend, predict and manipulate the microscopic world. By the end of the 20th century and start of the new millennium, the epoch's technological development made it possible to manipulate new concepts which were fundamental for the understanding of truly quantum phenomena. This way, terms like *superposition* and *entanglement* got the spotlights in the scientific world and the search for the development of new technologies that apply quantum effects intrinsic to the microscopic realm got impulsed. Development of more sensitive detectors, applications to communications networks and energy storage were some of the new targets during the so-called *second quantum revolution*, which extends up to the present days. In this thesis, we develop optimization methods for the charging of *quantum batteries*, which are microscopic systems fabricated with the goal of storing energy to be later used at some task of interest. We use the paradigm of quantum

open systems, which is the description furnished to microscopic systems that suffer from deleterious effects from the environment in which they are inserted. Here, we develop some techniques to use quantum resources present in the system (as quantum coherence, for instance) to optimize the charging process of such batteries.

Keywords: quantum battery; quantum open systems; quantum technologies; qubit; resonant cavities; quantum thermodynamics; gauge; symmetries; QED; quantum optics.

Agradecimentos

Já é consolidado para mim que a habilidade mais importante para um pesquisador é a capacidade de lidar bem com as próprias frustrações. Durante a graduação em física, onde tal habilidade começa a ser desenvolvida (e posta à prova simultaneamente), os jovens cientistas em formação, ainda que de forma inconsciente, se atentam a esse fato através de incontáveis ocasiões vividas durante curtíssimos quatro anos. Naturalmente, durante este período da formação, temos contato majoritariamente com aquilo que dá certo: o conjunto de conhecimentos que nos é apresentado já foi absorvido, aprendido, digerido e devolvido de maneira completamente esmiuçada por nossos antecessores e isto, por si só, já requer bastante empenho e dedicação destes últimos. A todos os professores que participaram do meu processo de formação e que de algum modo contribuíram para o meu aprendizado e interesse na área, os meus mais sinceros agradecimentos.

O próximo passo natural na formação do pesquisador, a pós-graduação e, em especial, o processo de doutoramento, é a etapa onde começa-se a ter contato com aquilo que não dá certo: cálculos enormes que perdem o sentido, interpretações falhas, incertezas sobre o grau de novidade do que se está pesquisando, entre outras micro situações que, imagino eu, não sejam dignas o suficiente pra se apresentarem em conversas de corredor. A vida acadêmica, afinal, é bastante solitária se comparada à maioria das outras áreas de trabalho no mundo moderno. Por tudo isto, o papel do orientador, e em especial do bom orientador, se faz importante no dia-a-dia do doutorando. Ao professor Marcelo França, por ter aceitado e executado com excelência o papel de orientador, e ter me acompanhado de perto ao longo dos quatro anos de doutoramento, o meu muito obrigado! É impossível a mim atribuir o devido valor à quantidade de coisas que aprendi sob sua orientação.

Finalmente, não é incomum, no meio acadêmico, a tendência ao isolamento. Afinal, como já disse anteriormente, é uma vida deveras solitária. Escapar dessa tendência, julgo, é a segunda habilidade mais importante para se manter ativo (e saudável) neste meio. Enquanto a primeira é exclusivamente auto desenvolvida, a segunda requer ingredientes externos dentre os quais, sem dúvida, o mais notório é a sorte. Felizmente, essa eu tenho bastante. Desde sempre tive o apoio do meu pai Ademilton e da minha mãe Célia, as conversas de almoço com minha avó Margarida, os domingos de churrasco com minha sogra Tânia, sempre consegui fazer bons colegas e ótimos amigos dentro e fora da academia, e em especial um seleto grupo de amigos do peito: à Amílcar Araújo, Gabriel Teixeira, Jade Maia, Juliana Carvalho, Osvaldo Ferreira, e Vicente Machado, um muítissimo obrigado pelo privilégio de ter a amizade diária de vocês. Por fim, à minha amada Úrsula Martins por me dar apoio e incentivo diário no nosso caminho em comum. É muito bom dividir com você um caminho dentro e fora da academia. Obrigado por ser minha companheira!

Este projeto de doutorado foi financiado com recursos públicos por meio da Coordenação de Aperfeiçoamento de Pessoal de Nível Superior (CAPES). Expresso meus profundos agradecimentos a esta e a todas as outras agências de fomento de pesquisa no Brasil, por exercerem papel fundamental na expansão e consolidação da pós-graduação no país.

Contents

Introduction

With the advent and development of quantum theory, a certain interest of its applications for practical purposes has been on the rise, specially from the early 1960 - 90's on what has been called the *first quantum revolution*. Marked by the first developments made using strictly quantum physics, this era was flagged by the creation of the first semiconductors, GPS, MRI techniques and the advent of the laser. The latter, for instance, has posed an enormous leap forward for many areas of physical sciences, since it has helped the further development of quantum optics on, for instance, the preparation and manipulation of photonic states [1–3] and enhanced techniques related to cavity QED [4,5]. These and other developments paved the way for the beginning of what today is known as the *second quantum revolution* [6, 7].

The second quantum revolution is a name that has been assigned to the developments of quantum theory applications where intrinsically quantum features are exploited in order to outperform regular classical tasks. In this paradigm, the development of the first quantum computers serve at least as a proof of principle that physical entities like coherence and entanglement, which are not present in macroscopic classical systems, can indeed serve as potent allies in the search for practical solutions to long standing problems which were proved to be unsolvable (at least on finite time) by classical computers [8–10].

This scenario has fostered a great endeavour, both theoretic and experimental, to propose and develop gadgets which could benefit from the so-called quantum resources [70–72]. This way, from prior to the beginning of the 21^{st} century up until the present days, the field of *quantum technologies* has attracted more and more research focused on

the studies about quantum sensors [14–17] (apparatus which explore quantum resources to enhance metrological quests on the fine-tuned estimation of physical parameters), the security of quantum communications [18–21] (establishing channels to send and receive messages which are truly inexpugnable), quantum energetics [22–26] (harnessing microscopic systems to store and manipulate energy which can be used on demand), to name a few.

On the scenario of quantum energetics, more specifically, the development of the first quantum computers has raised the interest for sources of energy that can be addressed on demand to fulfil desired physical tasks. This has fostered the development of the first prototypes of *quantum batteries*, which are gadgets aimed at storing and delivering specific amounts of energy (generally encoded in photon states) upon request. This piece of technology can meet applications in diverse platforms: from single atoms [27] and molecules [28], to extensive many-body condensed matter systems [29], quantum batteries meet various applications which target on protocols that can enhance their charging and discharging time [30,31], energetic storage capacity [32], stability [33], among other figures of merit that are dear if practical developments are to be achieved.

This thesis is inserted in the context just described. Especially, we hereafter focus on developing research about the applications of quantum theory to the field of quantum batteries. In this concern, we address typical issues which are present in this area: how can a microscopic system be employed to store energy? What is its maximum storage capacity? How can it be charged and is there a way to minimize its charging time? What are the important figures of merit to characterize a certain quantum battery? In addition to that, we also tackle more recent questions related to the exploitation of truly quantum resources in the charging of quantum batteries: are there strategies of charging that maximize some of the chosen figures of merit? If so, is there any detrimental physical quantity associated to the chosen strategy? How does the imperfect isolation of the battery to its surroundings impact its charging performance and stability? Can it be

explored in some way? These are some examples of the questions we have raised and try to respond to in the platforms we discuss throughout the scope of this thesis.

This thesis is organized as follows. In the first chapter we describe a quantum optical system developed to employ a three-level atom as a battery which needs to be charged by an external, classical power source. As an auxiliary, a quantized mode of the electromagnetic (EM) field interacts with the atom alone, and we explore this interaction to control the charging dynamics of the quantum battery. In most of the literature of cavity QED [34–36], which typically addresses this kind of system, the presence of the quantum vacuum of the EM field is actually detrimental, since it in general absorbs the excitations that would charge the battery. However, we design a protocol that can actually leverage on its presence, and presents better charging efficiency as the amount of vacuum increases. As the nature of this lowest-lying energy state of the EM field is intrinsically quantum, we compare our protocol with its classical counterpart which employs classical states of the EM field as auxiliary states for the charging of the atomic battery. By doing this, we show that our protocol indeed relies on the exploitation of the quantumness present in the vacuum state, and therefore constitutes a truly quantum protocol for charging the aforementioned battery.

In what follows, chapter two is dedicated to describe a natural follow-up of the previous protocol, but now exploring the role of quantum correlations. In a detailed description, we work with a collisional model where a sequence of similar three-level atoms interact with the same two modes of the EM field. The classical mode, still working as a power source, maximally charges the first atom in the chain, while leaving the quantum mode in the cavity in a specific final state. This final state interacts with the second atom, which evolves into a charged final state and thus updates the cavity's state. After a sequence of K such atoms, we investigate what is the final state of the quantum field, and evaluate the battery properties that it exhibits. Among other things, we show that there is an asymptotic capacity for the power charging of such hybrid system whenever

the atomic batteries' states are independent of each other. However, we also analyse the scenario where quantum and classical correlations are present within the global state of the chain, and show that, in this case, the asymptotic limit for the power charging is lifted, which renders a much more efficient charging for both quantum batteries. Finally, we also analyse whether the quantum nature of such correlations are indeed a resource for the charging in this case, and conclude with a comparison between the cases of an entangled global chain and a classically correlated one.

To top the results presented in this thesis, chapter three deals with a much more recent approach to the charging of quantum batteries. Namely, we investigate the effects of the environment in the evolution of a certain quantum system. Departing from a very general theory to describe open quantum systems, we analyse the reduced dynamics of the target system. Under this approach, the interaction between system and environment leads to correlations of both sets of degrees of freedom, and such correlations build up either weak or strong links between the states of both subsystems. Quantum decoherence naturally spoils these links, and in the asymptotic time domain both systems become fully uncorrelated. However, if one manages to read from the environment before the quantum correlations fade, it is possible to loosely guide the system through a sequence of probabilistic quantum jumps in its state. Therefore, choosing the appropriate set of environmental measurements may be harnessed as a possible resource to enhance some desired physical task and, in the final chapter, we address this topic by exploiting old and well-known symmetry properties of the Markovian master equation.

After all, we present a brief chapter summarizing the conclusions of the thesis and also introduce some of the follow-up research topics that eventually arise from our inquest.

Chapter 1

A simple model: QB inside a cavity

In this first chapter, we discuss an interesting model aimed at illustrating how one may leverage quantum phenomena to charge a quantum battery. The usefulness of the developed model, as we shall see, is that it meets straightforward applications in the field of resonant cavities [37–40] in quantum optics. Prior to that discussion, though, we must introduce in general grounds the basic notions behind the idea of using quantum systems to store useful energy. We do that briefly in the first section, when we define the notions of ergotropy [41, 42] and charging power, two figures of merit which are ubiquitous in the area of QBs. Then, in section two we pass straight to the discussion of the first results presented in this thesis, namely, the developed charging scheme aimed at exploring truly quantum phenomena for the charging of an atom when interacting with a mode of the electromagnetic field.

1.1 Quantum batteries

In the classical world, batteries are gadgets which explore chemical reactions to release a controlled amount of energy on demand. These can be disposable or rechargeable, depending on whether it is possible or not to invert the flow of energy by using external classical sources. Alternatively, its quantum counterpart stores the energy of photons rather than electrons or ions, as most of the theoretical platforms for realizing quantum

batteries are atomic. Additionally, a quantum battery may also rely on phenomena intrinsic to the microscopic realm, such as coherence or entanglement, in order to boost its figures of merit.

We start by considering a $d-$dimensional quantum system described by some density matrix ρ_0 and subjected to a set of interactions with other classical (*e.g.*, lasers or other macro states of the electromagnetic field) or quantum systems (*e.g*, atoms or quantized modes of the EM field). In general, this set of interactions performs some change $\rho_0 \to \rho_t$ in the state of the system, and some questions naturally arise: is this transformation raising or lowering the system's internal energy? If it is raising, can we extract it and, if so, how? Is there any kind of intervention we can do in order to reduce the amount of time which is necessary to achieve a certain amount of internal energy gained? Or, in other words, can we control the energetic *power* flowing into the system? These and other questions have been raised and answered in the literature for different platforms in an area that has been named as the *quantum batteries* research field. Most interestingly, trying to address these questions in a scenario where truly quantum phenomena can be harnessed to improve, for instance, the charging performance, is something that still holds the attention of many researchers in the field. For a thorough and up-to-date review on the topic, refer to Campaioli *et al*, 2024 [43].

In what follows, we briefly sketch the main goals for a protocol aimed at charging (*i.e.*, increasing the system's internal energy), as well as discharging (retrieving the stored amount of energy on demand).

1.1.1 Charging and discharging

In general, a QB may be charged under two different protocols: unitary or dissipative charging [44], each one with its own subtleties and limitations. In the first case, the system which serves as the energy storage coherently interacts with a secondary quantum or classical system, which leads into a closed evolution for the combined battery + charger

system. In this case, the charging protocol is stopped whenever some desired figure of merit is achieved. Alternatively, the QB may also be subjected to an incoherent interaction with some environment, generically treated as an unknown system, such that its open quantum evolution now irreversibly changes its state. Again, the protocol is stopped whenever some threshold for, *e.g.*, the internal energy, is achieved. In most of the recent developments of quantum batteries a combined coherent and incoherent [45,46] evolution is engineered in order to explore richer physical phenomena in the charging process.

In the cases we shall be interested throughout this thesis, the most general evolution for the QB's quantum states will be Markovian and given by the celebrated Lindblad master equation, which reads

$$\frac{d\rho}{dt} = -i\left[\hat{H}, \rho\right] + \sum_{i=1}^{N} L_i \rho L_i^\dagger - \frac{1}{2}\{L_i^\dagger L_i, \rho\}, \tag{1.1}$$

where L_i are Lindblad operators that act on the system as back actions of the environmental degrees of freedom constantly measuring the state of the former. Furthermore, $\hat{H}$ is the effective Hamiltonian leading the coherent part of the evolution, which is essentially composed by the system's free Hamiltonian $\hat{H}_0$ (*i.e.*, its energy operator when it is isolated) as well as external drive contributions $\hat{H}_d$ (in general, classical states of the electromagnetic field).

For a certain state ρ_A to be considered as the fully charged state of a quantum battery, one must be able to extract the stored energy in a controlled fashion, *i.e.*, with deterministic knowledge regarding the total extraction time, which must be finite, and the total extracted energy at the end of the thus named *discharging* process. It turns out that, with such requirement, the system's internal energy is not the most appropriate figure of merit to characterize the battery's energetic capacity any more.

Instead, Allahverdyan *et al* [47] have defined the concept of *ergotropy* as the maximum amount of energy that can be extracted from a quantum system under a unitary operation, *i.e.*:

$$\mathcal{E}\left(\rho_A, \hat{H}\right) \equiv \max_{U \in SU(d)} \mathrm{Tr}\left(\rho_A \hat{H}\right) - \mathrm{Tr}\left(U \rho_A U^\dagger \hat{H}\right) \overset{!}{>} 0. \tag{1.2}$$

Notice that this is a real functional solely of the $d-$dimensional system's density matrix ρ_A and of its Hamiltonian $\hat{H}$. Furthermore, U is the unitary transformation which extracts the ergotropy, optimized over all possible elements of $SU(d)$, provided that $\mathrm{Tr}\left(\rho_A \hat{H}\right) > \mathrm{Tr}\left(U \rho_A U^\dagger \hat{H}\right)$, which is reminded in the definition by the exclamation mark (!).

The reasoning behind this definition is straightforward: consider, for example, the family of states $\sigma_\delta = (1-\delta)|g\rangle\langle g| + \delta|e\rangle\langle e|$, defining possible states for a two-level system with Hamiltonian $\hat{H} = \omega|e\rangle\langle e|$. Their internal energy reads $\langle \hat{H} \rangle_{\sigma_\delta} = \omega\delta$. It is possible to show, as we will soon discuss, that the U which maximizes the unitary energy extraction in this case is given by $U = |g\rangle\langle e| + |e\rangle\langle g|$. By applying this U to σ_δ we achieve the population swapped state $U\sigma_\delta U^\dagger = (1-\delta)|e\rangle\langle e| + \delta|g\rangle\langle g|$ with internal energy $\langle \hat{H} \rangle_{U\sigma_\delta U^\dagger} = \omega(1-\delta)$. The ergotropy is, therefore, given by $\mathcal{E}(\sigma, \hat{H}) = \omega(2\delta - 1)$, which is strictly positive only for half of the family $\delta > 1/2$. This means that only the states σ_δ with $\delta > 1/2$ store ergotropy, even though the whole family possesses non-null internal energy (except, in this case, for $\delta = 0$).

The catch is that the states σ_δ for $\delta < 1/2$ can only lose energy through non-unitary processes, such as spontaneous emission for instance, and since these kinds of processes are stochastic instead of deterministic, one cannot control with certainty when this amount of energy will be available. From this comes the need of defining ergotropy, rather than internal energy, as the main figure of merit of a quantum battery.

1.1.2 Extraction unitary and passive states

Once the battery's charged state ρ_A is achieved after the charging process, one's task is to find the best way to extract the stored ergotropy via a unitary transformation U. By definition, U must be an operator which takes ρ_A to $\rho_P = U\rho_A U^\dagger$ such that ρ_P has zero

ergotropy left to be extracted. We name ρ_A as the *active* battery state, while ρ_P is the *passive* state associated to ρ_A. This realization leads to the conclusion that there is a one-to-one correspondence between active and passive states, in the sense that, up to an imaginary phase, there is a unique unitary U which fully extracts the stored ergotropy. In what follows we shall quickly derive this unitary.

Let us start by assuming as Hamiltonian the operator $\hat{H} = \sum_j \epsilon_j |\epsilon_j\rangle\langle\epsilon_j|$ with eigenvalues in increasing order, *i.e.*, $\epsilon_{i+1} \geq \epsilon_i$. Also, we work with the spectrally decomposed form of the active state's density matrix $\rho_A = \sum_i p_i |p_i\rangle\langle p_i|$. According to definition (1.2), the unitary U which furnishes the maximum extracted energy must be the one to minimize the factor $\mathrm{Tr}\left(U\rho_A U^\dagger \hat{H}\right)$. This means that once U is found, any variation δU must not alter the passive state's internal energy, *i.e.*, $\delta E(\rho_A) = \mathrm{Tr}\left(\delta U \rho_A U^\dagger \hat{H} + U\rho_A \delta U^\dagger \hat{H}\right) = 0$. Once that δU can always be parametrized as $\delta U = XU$, for some anti-hermitian operator X ($X^\dagger = -X$), we find

$$\delta E(\rho_A) = \mathrm{Tr}\left(X[U\rho_A U^\dagger, \hat{H}]\right) = 0. \tag{1.3}$$

Since X is an arbitrary parameter, the only way to guarantee this extremity is if $\rho_P = U\rho_A U^\dagger$ and $\hat{H}$ commute, *i.e.*, if the discharged density matrix can be diagonalized in the energy eigenbasis. The most general unitary to perform a transformation from $|p_i\rangle\langle p_i|$ to $|\epsilon_i\rangle\langle\epsilon_i|$ is $U = \sum_j |\epsilon_j\rangle\langle p_j|$.

It can be checked that this unitary does not alter the ordering of the eigenvalues of ρ_A, *i.e.*, if, for instance $p_3 > p_4 < p_5$ in ρ_A, then it is also true for ρ_P. An optimal active state $\rho_A = \sum_i p_i |p_i\rangle\langle p_i|$ must be such that its most energetic eigenstates (with mean energy given by $\langle p_i| \hat{H} |p_i\rangle$) must possess the highest populations p_i. On the other hand, since this is not generally true, we must first reorder the eigenvalues and eigenvectors of ρ_A in order to guarantee that the extraction unitary transfers the maximum amount of population to the lowest lying energetic states. We therefore find that the optimal unitary to fully extract the system's ergotropy upon discharging is given by

$$U = \sum_j |\epsilon_j\rangle\langle p_j^{dec}|, \tag{1.4}$$

where p_j^{dec} are the eigenvalues of ρ_A ordered decreasingly $p_i > p_{i+1}$. Applying this unitary to (1.2) we find the explicit expression for the ergotropy, in terms of the Hamiltonian and the already ordered eigenbasis of ρ_A:

$$\mathcal{E}\left(\rho_A, \hat{H}\right) = \sum_i p_i^{dec}\left(\langle p_i^{dec}|\,\hat{H}\,|p_i^{dec}\rangle - \epsilon_i\right). \tag{1.5}$$

By this simple reasoning we find that, despite its logical simplicity, the ergotropy is highly dependent on the eigenbasis difference between the system's density matrix and its Hamiltonian. This, in turn, is explored by different protocols that focus on either changing the system's Hamiltonian or the active state (or both) in order to boost the ergotropy by exploring, for instance, energetic coherences present in a certain dynamics. [48–51]

1.1.3 Extending on qubits: the role of purity

One of the simplest models for realizing a quantum battery is a two-level system (TLS). In spite of its low dimensionality, TLS are very useful in a wide variety of practical applications due to the small amount of control parameters and the facility to engineer their interactions with external drives. Be it on spin chains, Rydberg atoms or other physical systems, a qubit is the simplest model for a QB. In this subsection we explicitly calculate, as a straightforward example, the ergotropy for this kind of system.

We consider a general state $\rho_A = \delta|e\rangle\langle e| + (1-\delta)|g\rangle\langle g| + c|e\rangle\langle g| + c^*|g\rangle\langle e|$ subject to the Hamiltonian $\hat{H} = \frac{\omega}{2}\hat{\sigma}_z$ in which $\epsilon_1 = -\frac{\omega}{2} < \epsilon_2 = \frac{\omega}{2}$. Once again, $\delta \leq 1$ is the population of the $|e\rangle$ state, but now we also allow for the presence of energetic coherences c. Naturally, the coherences are such that $|c| \leq \sqrt{\delta(1-\delta)}$, with the equality holding if ρ_A is a pure state.

In order to calculate the ergotropy, one must find the spectral decomposition of ρ_A, whose eigenvalues are given by

$$p_{\pm}^{dec} = \frac{1}{2} \pm \Delta, \tag{1.6}$$

with $\Delta = \sqrt{(\delta - \frac{1}{2})^2 + |c|^2}$. Furthermore, the eigenstates associated to these populations are given by $|p_{\pm}^{dec}\rangle = \alpha_{\pm} |e\rangle + \beta_{\pm} |g\rangle$ where

$$\alpha_{\pm} = \frac{|c|}{\sqrt{(p_{\pm}^{dec} - \delta)^2 + |c|^2}}, \tag{1.7}$$

$$\beta_{\pm} = \frac{e^{i\theta}(p_{\pm}^{dec} - \delta)}{\sqrt{(p_{\pm}^{dec} - \delta)^2 + |c|^2}}. \tag{1.8}$$

Here, $\theta = arg(c)$. With these results and equation (1.5), we have:

$$\mathcal{E}\left(\rho_A, \hat{H}\right) = \left(\frac{p_{+}^{dec}|c|^2}{(p_{+}^{dec} - \delta)^2 + |c|^2)} - \frac{p_{-}^{dec}(p_{-}^{dec} - \delta)^2}{(p_{-}^{dec} - \delta)^2 + |c|^2)}\right)\omega, \tag{1.9}$$

which can be simplified, after some algebraic manipulations, to

$$\mathcal{E}\left(\rho_A, \hat{H}\right) = \left(\Delta + \delta - \frac{1}{2}\right)\omega, \tag{1.10}$$

with ω the energy gap of the qubit.

Parallel to that, the active states purity can be calculated as

$$P_A = \mathrm{Tr}\left(\rho_A^2\right) = p_{+}^2 + p_{-}^2 = \frac{1}{2} + \frac{4\Delta^2}{2}, \tag{1.11}$$

while the internal energy is

$$U_A = \mathrm{Tr}\left(\rho_A \hat{H}\right) = \left(\delta - \frac{1}{2}\right)\omega. \tag{1.12}$$

These two expressions allow us to write the final form for the qubit's ergotropy as

$$\mathcal{E}\left(\rho_A, \hat{H}\right) = \left[\frac{\sqrt{2P_A - 1}}{2}\right]\omega + U_A, \tag{1.13}$$

which makes clear that there are two main contributions for an arbitrary qubit quantum battery's ergotropy.

Firstly, the purity of the active state plays an essential role in raising its stored ergotropy, which is evident by the form of the first bracketed term. This factor is lower bounded by 0 for a maximally mixed state, and upper bounded by $\omega/2$ for a pure state. Since this maximum is only achieved for pure states, it is always desirable to seek charging protocols that purify the battery's final state. However, the second factor also plays a role in determining the system's stored ergotropy, since the internal energy of a qubit is not a positive definite quantity with the given Hamiltonian.

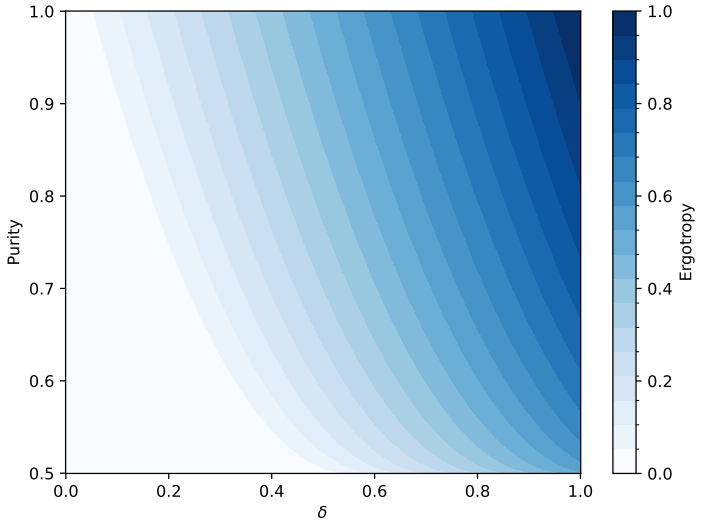

Figure 1.1: The role of purity for a qubit QB's ergotropy. Even for small purity states, we meet non-zero values of ergotropy in the $\delta \leq 1/2$ region, which is a forbidden zone for maximally mixed states.

This interplay between internal energy and purity for a qubit's ergotropy can be graphically seen on Figure 1.1. Here, we plot $\mathcal{E}/\omega$ as a function of the excited population δ and the active state's purity. We see that, even for small purity we have non-zero ergotropy in the region $\delta \leq 1/2$, which therefore establishes the purity present in the QB's state as useful resource in the extraction process.

1.2 EM field as a charger

(*Phys. Rev. A 107, 032203*)

After a brief introduction to the basic concepts which shall be used in the rest of this thesis, we now proceed to discuss the first contribution achieved for the field of quantum batteries. In this section, we carry a detailed discussion on how the interaction between an atomic system (the quantum battery) and a mode of the electromagnetic field in a cavity (the charger) can be harnessed in order to boost the charging performance of the QB.

1.2.1 The model

We start by considering the interaction of a three-level system (qutrit) with a mode of the electromagnetic field inside a cavity. As we shall see, under some specific conditions related to the couplings involved, the most energetic level of the qutrit can be adiabatically eliminated from the dynamics and we are left with an effective two-dimensional system, which is going to be the qubit used as a QB. We analyse the two cases where the charger is either in a classic or a quantum state of the EM field, and show that the quantum version presents true advantages due to the presence of the quantum vacuum.

Figure 1.2 shows the whole interaction scheme: a classical mode ω_L of the EM field, which acts as a power source, off-resonantly couples the $|g\rangle \leftrightarrow |m\rangle$ transition with coupling Ω_L; parallel to that, another quantum (classical) mode ω_q couples, also off-resonantly, the $|e\rangle \leftrightarrow |m\rangle$ transition with coupling constant g (Ω_R).

The Hamiltonian for this system is given either by

$$\hat{H}_{cl} = \sum_{j=g,e,m} \omega_j |j\rangle\langle j| + \Omega_L \left(\hat{\sigma}_{gm} e^{i\omega_L t} + \hat{\sigma}_{mg} e^{-i\omega_L t}\right) + \Omega_R \left(\hat{\sigma}_{em} e^{i\omega_q t} + \hat{\sigma}_{me} e^{-i\omega_q t}\right), \quad (1.14)$$

or

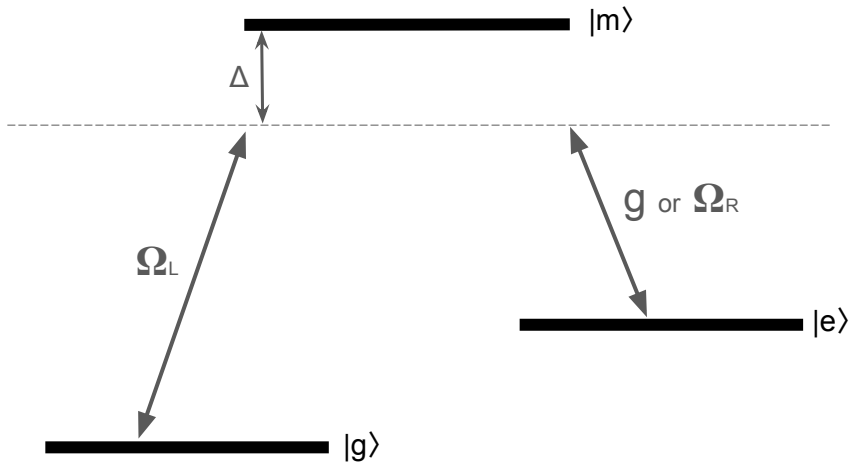

Figure 1.2: Energy levels scheme between a classical power source (left) and a quantum or classical mode of the EM field (right). The classical mode Ω_R is considered solely as a benchmark to which we compare how advantageous the quantumness of the vacuum of the EM field is.

$$\hat{H}_{qu} = \sum_{j=g,e,m} \omega_j |j\rangle\langle j| + \omega_q \hat{a}^\dagger \hat{a} + \Omega_L \left(\hat{\sigma}_{gm} e^{i\omega_L t} + \hat{\sigma}_{mg} e^{-i\omega_L t}\right) + g\left(\hat{\sigma}_{em}\hat{a}^\dagger + \hat{\sigma}_{me}\hat{a}\right), \quad (1.15)$$

where $\hat{\sigma}_{ij} = |i\rangle\langle j|$ and $\hat{a}, \hat{a}^\dagger$ are the usual ladder operators for the qutrit and EM field, respectively. Here, $\hat{H}_{cl}$ describes the ordinary Raman coupling between the qutrit and two classical modes of frequencies ω_L and ω_q, and $\hat{H}_{qu}$ represents the coupling between the qutrit with both a classical and a quantum mode of the electromagnetic field. In what follows, we use the former system as a benchmark, while the latter is analysed and used in our protocol to discuss the advantages arising from the quantization of the EM mode ω_q.

Moving to the interaction picture, $\hat{H}_{qu}$ changes to the interaction Hamiltonian given by

$$\hat{H}_{int} = \Omega_L \left(\hat{\sigma}_{mg} e^{i\Delta t} + \hat{\sigma}_{gm} e^{-i\Delta t}\right) + g\left(\hat{\sigma}_{me}\hat{a}e^{i\Delta t} + \hat{\sigma}_{em}\hat{a}^\dagger e^{-i\Delta t}\right). \quad (1.16)$$

Naturaly $\Delta = \omega_{mg} - \omega_L = \omega_{me} - \omega_q$, with $\omega_{ij} = \omega_i - \omega_j$. Since both transitions

$|g\rangle \leftrightarrow |m\rangle$ and $|e\rangle \leftrightarrow |m\rangle$ are dipole coupled, direct population transfer between levels $|g\rangle$ and $|e\rangle$ is forbidden by selection rules. However, if the couplings Ω_L, g are weak enough or, conversely, if the detuning Δ is wide enough, then (1.16) describes a fast oscillating dynamics for which the net effect is to transfer population from $|g\rangle$ to $|e\rangle$ through $|m\rangle$, *i.e.*, level $|m\rangle$ only serves as an ancilla to virtually transfer excitations in the $|g\rangle \leftrightarrow |e\rangle$ subspace. This can be seen by taking the time average of (1.16), following the main result of reference [52]. In the regime where $\Delta \gg \Omega_L, g$, the time-averaged, effective Hamiltonian is

$$\tilde{H}_{eff} = -\frac{\Omega_L^2}{\Delta}\hat{\sigma}_{gg} - \frac{g^2\hat{a}^\dagger\hat{a}}{\Delta}\hat{\sigma}_{ee} - \frac{g\Omega_L}{\Delta}\left(\hat{\sigma}_{eg}\hat{a}^\dagger + \hat{\sigma}_{ge}\hat{a}\right) + \left(\frac{\Omega_L^2}{\Delta} + \frac{g^2}{\Delta}(\hat{a}^\dagger\hat{a}+1)\right)\hat{\sigma}_{mm}. \quad (1.17)$$

Indeed, as we see in the last term of (1.17), in this regime the evolution for the population of $|m\rangle$ decouples from the $|g\rangle, |e\rangle$ levels and we have $\dot{p}_m(t) = 0$, meaning that if initially level $|m\rangle$ has no population, it remains unpopulated on average. Moreover, we find that the effective energy difference between the two levels of the qubit $\hbar\tilde{\omega}_{eg} = \hbar\dfrac{\Omega_L^2 - g^2 n_f}{\Delta}$ depends on the number n_f of excitations present in the cavity field. To simplify our analysis, we add a small correction to the energy of level $|g\rangle$ by means of a d.c. Stark shift $\Delta_g^{N_0} = \dfrac{\Omega_L^2 - g^2 N_0}{\Delta}$, with N_0 a natural number, such that the final Hamiltonian describing our quantum battery two-level system + charger is

$$\hat{H}_{QB} = -\frac{g^2 N_0}{\Delta}\hat{\sigma}_{gg} - \frac{g^2\hat{a}^\dagger\hat{a}}{\Delta}\hat{\sigma}_{ee} - \frac{g\Omega_L}{\Delta}\left(\hat{\sigma}_{ge}\hat{a} + \hat{\sigma}_{eg}\hat{a}^\dagger\right). \quad (1.18)$$

This effective coupling between levels $|g\rangle$ and $|e\rangle$ is in an anti-Jaynes-Cummings configuration, in which the system atom+field absorb or emit two excitations collectively. This Hamiltonian is block-diagonal in the subspaces $\{|e,0\rangle, \{|g,n\rangle, |e,n+1\rangle\}\}$, for $n \geq 0$. Naturally, $|e,0\rangle$ is an eigenstate of $\hat{H}_{QB}$ with vanishing eigenvalue, which can be promptly checked from (1.18). The other eigenstates are given by

$$|\pm, n\rangle = \frac{G_n |g, n\rangle - E_\pm |e, n+1\rangle}{\sqrt{G_n^2 + E_\pm^2}}, \tag{1.19}$$

with $G_n = \frac{g\Omega_L}{\Delta}\sqrt{n+1}$, $\Omega_n = \sqrt{\frac{\Delta_n^2}{4} + G_n^2}$ the Rabi frequency of the $n-$doublet, and $\Delta_n = \frac{g^2}{\Delta}(n+1-N_0)$. Also, the eigenenergies are given by $E_\pm = \frac{\Delta_n}{2} \pm \Omega_n$. This is enough to find the evolution operator $U(t,0)$ for the whole system, which furnishes

$$U(t,0)\,|g,n\rangle = e^{-i\frac{\Delta_n t}{2}}\left[\left(\cos(\Omega_n t) + \frac{i\Delta_n}{2\Omega_n}\sin(\Omega_n t)\right)|g,n\rangle + \frac{iG_n}{\Omega_n}\sin(\Omega_n t)\,|e,n+1\rangle\right], \tag{1.20}$$

$$U(t,0)\,|e,n+1\rangle = e^{-i\frac{\Delta_n t}{2}}\left[\frac{iG_n}{\Omega_n}\sin(\Omega_n t)\,|g,n\rangle + \left(\cos(\Omega_n t) - \frac{i\Delta_n}{2\Omega_n}\sin(\Omega_n t)\right)|e,n+1\rangle\right]. \tag{1.21}$$

1.2.2 Selectivity and figures of merit

We are interested in the case where no energetic coherence is present either on the battery's or the charger's initial state, *i.e.*, it is of the form

$$\rho(0) = \sum_{i=g,e,m} r_i |i\rangle\langle i| \otimes \sum_{n=0}^{\infty} p_n |n\rangle\langle n|. \tag{1.22}$$

As it can be straightforwardly checked, from this initial state no energetic coherence is created on either systems. The evolution for the $n-$doublet $\{|g,n\rangle, |e,n+1\rangle\}$ is given by

$$\langle g,n|\,\rho(t)\,|g,n\rangle = r_g p_n - \frac{G_n^2}{\Omega_n^2}(r_g p_n - r_e p_{n+1})\sin^2(\Omega_n t), \tag{1.23}$$

$$\langle e,n+1|\,\rho(t)\,|e,n+1\rangle = r_e p_{n+1} + \frac{G_n^2}{\Omega_n^2}(r_g p_n - r_e p_{n+1})\sin^2(\Omega_n t). \tag{1.24}$$

In order to analyse this dynamics, we rewrite the G_n^2/Ω_n^2 factor as

$$\delta_n^2 \equiv \frac{G_n^2}{\Omega_n^2} = \frac{1}{1+\frac{r^2}{4}\frac{(N_0-n-1)^2}{n+1}}, \tag{1.25}$$

with $r \equiv g/\Omega_L$ the *selectivity ratio*. Whenever $g \gg \Omega_L$ ($r \gg 1$) this factor is vanishingly small for all n except $n = N_0 - 1$ and, therefore, all the doublets with $n \neq N_0 - 1$ are decoupled from the dynamics and do not evolve in time. Therefore, the regime $r \gg 1$ is named the *selective* regime, since for this case only the states $\{|g, N_0 - 1\rangle, |e, N_0\rangle\}$ evolve in time. Naturally, we pick which doublet is effectively coupled to the dynamics by changing the value of N_0 in the d.c. shift applied to the atom. Alternatively, the $r \ll 1$ is called the *non-selective* regime, where all the doublets evolve with different Rabi frequencies.

By taking the partial trace over the charger's degrees of freedom, we find the evolution of the battery's energy levels as

$$\rho_{QB}(t) = \rho_{QB}(0) + S(t)\left(|e\rangle\langle e| - |g\rangle\langle g|\right), \tag{1.26}$$

with the function $S(t)$ given by

$$S(t) = \sum_{n=0}^{\infty} S_n = \sum_{n=0}^{\infty} \frac{G_n^2}{\Omega_n^2}(r_g p_n - r_e p_{n+1}) \sin^2(\Omega_n t). \tag{1.27}$$

Furthermore, the variation of internal energy and the ergotropy of the system are given respectively by

$$\Delta U_{QB}^q(t) = \hbar\omega_{eg} S(t), \tag{1.28}$$

$$\mathcal{E}_{QB}^q(t) = \hbar\omega_{eg}[r_e - r_g + 2S(t)], \tag{1.29}$$

where the last equality holds for times t which furnish positive values for the ergotropy.

As previously said, we use the model given by Hamiltonian (1.14) as benchmark. This consists of two classical modes of the electromagnetic field coupled in a Raman setting

to the qutrit. After adiabatic elimination under the same conditions of the quantum protocol, we find that the best case scenario for this benchmark occurs whenever there is a total population swap between the ground and excited levels, in which case the variation in internal energy of the battery is

$$\Delta U_{QB}^{cl} = \hbar\omega_{eg}(r_g - r_e). \tag{1.30}$$

Since the classical charging scheme is unitary, the purity present in the initial state of the battery does not change, and therefore this variation in the internal energy also corresponds to the ergotropy $\mathcal{E}_{QB}^{cl}$ gained in the battery by the fully classical protocol. Therefore, by means of equations (1.28), (1.29) and (1.30), we find that exploiting the quantumness of the electromagnetic field is only advantageous whenever $\mathcal{E}_{QB}^{q} - \mathcal{E}_{QB}^{cl} = 2(\Delta U_{QB}^{q} - \Delta U_{QB}^{cl}) > 0$, *i.e.*, we may use the variation in the internal energy as a figure of merit since it is directly related to the gains in ergotropy. For this, we define the relative energetic gain K_q as

$$K_q = \frac{\Delta U_{QB}^{q} - \Delta U_{QB}^{cl}}{\Delta U_{QB}^{cl}}. \tag{1.31}$$

1.2.3 Vacuum enhanced charging

First of all, there are two immediate limits which can be used to tackle the designed charging protocol. The first relates to taking the initial state of the electromagnetic field as a coherent state with large average number of photons $\overline{n}$. In this scenario, the initial populations of the field are given by a Poisson distribution which is commonly called a *semi-classical* distribution for the EM field. In this case, the protocol inverts the atomic population and $K_q \to 0$ as the quantum protocol retrieves the classical results in the $\overline{n} \gg 1$ limit.

Alternatively, a second regime of operation is the zero-temperature regime ($T = 0$). In this case we have $r_g = p_0 = 1$, and it is straightforward to evaluate that (1.27) is maximal

at a $\pi-$flip $\Omega_0 t = \pi/2$, in which case the field is also performing a population inversion of the atomic levels and $K_q = 0$.

The most interesting scenario arises in the more realistic case of both battery and charger initially in thermal equilibrium with a finite temperature reservoir ($T > 0$). In this case, the Gibbs distributions for the battery and charger are, respectively

$$r_i = \frac{e^{-\beta\hbar\omega_i}}{Z_{QB}}, \tag{1.32}$$

$$p_n = \frac{e^{-\beta\hbar\omega_q n}}{Z_{ch}}, \tag{1.33}$$

with $i = g, e, m$, $Z_{QB} = e^{-\beta\hbar\omega_e} + e^{-\beta\hbar\omega_g} + e^{-\beta\hbar\omega_m}$ and $Z_{ch} = \dfrac{1}{1 - e^{-\beta\hbar\omega_q}}$. Here, $\beta = \frac{1}{k_B T}$ is the inverse initial temperature of the joint initial state.

The optimal charging protocol hinges on the limit $r \gg 1$ (*i.e.*, the selective regime). In this regime, we initially set the detuning parameter $N_0 = 1$, in which case the only doublet which is resonant is the $\{|g,0\rangle, |e,1\rangle\}$, while any other $n > 1$ is detuned by a quantity Δ_n much larger than the coupling constant G_n. In this case δ_n^2 approximately equals the Kronecker's delta $\delta_{n,0}$, and the function $S(t)$ simplifies to $S(t) = (r_g p_0 - r_e p_1)\sin^2(\Omega_0 t)$, which is maximal at a time τ_1 such that $\Omega_0\tau_1 = \pi/2$. The total system's state is given at this time by

$$\begin{aligned}\rho(\tau_1) \;&= r_e p_0 |e,0\rangle\langle e,0| \;+\; r_g p_0 |e,1\rangle\langle e,1| \;+\; r_e p_1 |g,0\rangle\langle g,0| \\ &+ r_g p_1 |g,1\rangle\langle g,1| \;+\; \left(\rho_{at}(0) \otimes \sum_{n>1} p_n |n\rangle\langle n|\right).\end{aligned} \tag{1.34}$$

Now, a new detuning $N_0 = 2$ is selected, transferring population in the doublet $|g,1\rangle \to |e,2\rangle$ and leaving the remaining probabilities untouched. Repeating the mechanism for $N_0 = j + 1$ ($j = 1, 2, ...$), and adjusting the interaction time τ_{N_0} at each detuning, the battery state evolves to $\rho\left(\sum_j \tau_{j+1}\right) = [r_e(1 - p_0)]|g\rangle\langle g| + (r_g + r_e p_0)|e\rangle\langle e|$, with $\Delta U^q_{QB} = \Delta U^c_{QB} + \hbar\omega_{eg} r_e p_0$, *i.e.*, the protocol with the quantized electromagnetic field is

always advantageous. Note that, in the limit $\hbar\omega_q \gg k_B T$, we have $p_0 \to 1$ and the battery achieves full charge regardless of its initial state. This is a purely quantum effect due to the vacuum of the electromagnetic field.

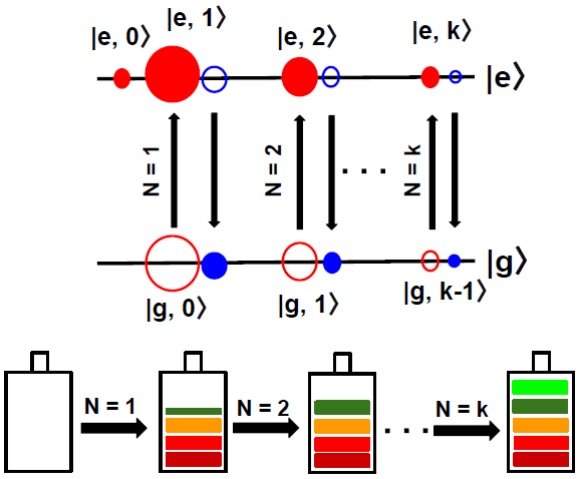

Figure 1.3: General scheme of multi-shot charging by sequential changing of the detuning. This protocol completely charges the qubit used as battery by exploiting the presence of the quantum vacuum of the charger. It shows a real quantum advantage in the charging process of an atomic battery.

Figure 1.3 shows the described charging scheme as a sequence of detuning adjustments on the value of N_0. In the low-temperature regime for the charger, most of the energy input in the battery comes from the lowest lying values of detuning, since the most of the population of the charger states are accumulated in the neighbourhood of the vacuum level.

Despite its effectiveness in completely charging the battery, *i.e.*, leaving the atomic state at the $|e\rangle$ eigenstate, this protocol is somewhat cumbersome to be practically implemented. Firstly, each detuning $N_0 = j+1$ must be applied during a doublet-charging time $\tau_{j+1} = \frac{\pi}{2\Omega_j}$, with $\Omega_j = \frac{g\Omega_L}{\Delta}\sqrt{j+1}$ the Rabi frequency of the doublet being pumped. For instance, if we have $\Delta = 2\pi\cdot$MHz, $g = \Delta/20$ and $\Omega_L = \Delta/600$ (such that $r^2 = 900 \gg 1$), we find $\tau_{j+1} = \frac{3}{\sqrt{j+1}} \cdot 10^{-3}$ s. For most of physical applications, this is longer than the decoherence time of the atom [53]. Therefore, we ought to investigate the effects on charging

where only a single detuning is considered. In addition to that, it is also relevant to quantify the charging scheme under environmental dissipation conditions. In what follows, we do these two investigations and analyse the relative energetic gain figure of merit.

1.2.4 Single-shot scenario

In order to faithfully compare our proposed charging protocol with the classical Raman charging by two classical fields, we must keep the total charging time under similar circumstances. In the classical protocol, the effective Rabi frequency of oscillation due to the Ω_L and Ω_R classical fields coupled is $\tilde{\Omega} = \frac{1}{2}\frac{\Omega_L^2+\Omega_R^2}{\Delta}$ and the total $\pi-$flip occurs at a time $\tau_{cl} = \frac{\pi}{2\tilde{\Omega}}$. This is commensurate with a single detuning $N_0 = 1$.

Under this restriction, we may wonder if the selective regime is indeed the most effective for charging. It turns out that it is not, which can be seen on Fig. 1.4. This is physically attributed to the fact that, under a fixed evolution time, letting all doublets evolve in parallel retrieves more energy than letting a single one. In this subsection, we collect these results and compare both regimes of operation for single-shot scenarios.

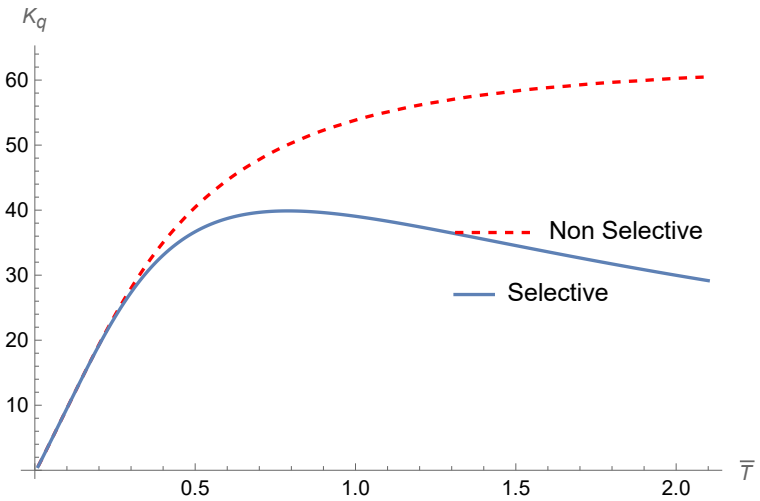

Figure 1.4: For low enough temperatures, only the lowest lying energy levels of the quantum field are populated. In this regime, both selective and non-selective regimes achieve similar gains. On the other hand, as the temperature increases it is the non-selective regime that achieves the best performance in the single-shot charging protocol. In the figure, the quantum-to-classical relative energy gain is plotted as a function of the dimensionless temperature $\overline{T} = k_B T/\hbar\omega_m$.

For the selective regime, the best adjustment is $N_0 = 1$, corresponding to state (1.34) for which $\Delta U^q_{QB} = \hbar\omega_{eg}(r_g p_0 - r_e p_1)$, achieved at a time $\tau_1 = \frac{\pi}{2\Omega_0}$. In this case, a simple calculation shows that $K_q \propto \Delta U^q_{QB} - \Delta U^{cl}_{QB} = \hbar\omega_{eg}\left[r_e(1-p_1) - r_g(1-p_0)\right]$ is only positive, and the quantum version advantageous, whenever $\frac{r_e}{r_g} > \frac{1-p_0}{1-p_1}$. Interestingly, there is an intermediate range of temperatures for which this condition is always satisfied: when $k_B T \ll \hbar\omega_q, \hbar\omega_m$ (but still commensurate with $\hbar\omega_{eg}$) the field is predominantly in the two lowest lying levels (*i.e.*, $p_n \approx 0$ for $n > 1$) and the atom's population is distributed only through the $|g\rangle, |e\rangle$ levels (*i.e.*, $r_m \approx 0$).

In this case we have $1 - p_1 \approx p_0$ and $1 - r_e \approx r_g$, and the condition for the positivity of K_q translates to $\frac{r_e p_0}{r_g p_1} \approx e^{\beta\hbar\omega_{eg}(\xi-1)} > 1$, where $\xi \equiv \frac{\omega_q}{\omega_{eg}}$. Naturally, K_q is only positive if $\xi > 1$, *i.e.*, whenever the atomic gap is smaller than the energy of the photon of the charger. In principle, the larger the value of ξ, the more accentuated the enhancement due to the vacuum of the quantum field. Moreover, in this regime, $\tilde{H}_{eff}$ approximately implements a swap between the states of the atom and the quantum field, leaving the battery in the state $\rho_{QB}(\tau) = p_0\hat{\sigma}_{ee} + p_1\hat{\sigma}_{gg} + r_m\hat{\sigma}_{mm}$, whereas the $\pi-$flip carried by the classical protocol generates $\rho_{QB}(\tau) = r_g\hat{\sigma}_{ee} + r_e\hat{\sigma}_{gg} + r_m\hat{\sigma}_{mm}$. These results, transparent in the selective regime of operation, shows that as long as the thermal probability of the ground state of the quantum field is larger than that of the ground state of the atom, the quantum protocol will present gain over the classical benchmark protocol. This is a purely quantum effect due to the quantum vacuum of the electromagnetic field, still present in the single-shot scenario.

However, as previously commented, $r \gg 1$ is not the optimal regime. A quick inspection of $S(t)$ in equation (1.27) shows that it is the opposite regime $r \ll 1$ that optimizes the energy transfer to the atom. In this case, there will be an almost resonant transference of population in all the doublets. The first term $S_1(t)$ already corresponds to the gain analysed in the selective regime, which is now augmented by the contributions of the remaining terms: since p_n is always larger than p_{n+1} for a Gibbs state, each doublet will

contribute positively to enhance the effect of the quantized field on the charging of the battery.

Because each doublet oscillates at a different Rabi frequency, it is impossible to choose a time interval τ_q that simultaneously maximizes the energy transfer in all of the doublets and the optimal interaction time, which naturally depends on the temperature T defining the initial states, has to be numerically extracted by maximizing $S(t)$. Because higher excited states oscillate faster, the optimal τ_q gets shorter for higher temperatures. Nevertheless, as expected, the relative gain K_q induced by the quantized field increases with T.

1.2.5 Purification in the single-shot scenario

As the general result for qubits suggest, achieving higher levels of state purification in the our protocol is desirable for enhancing its stored ergotropy. In this subsection we present some results related to the evolution of the QB's purity. This is defined as

$$P(t) \equiv \mathrm{Tr}\left(\rho_{QB}^2(t)\right) = P(0) + 2S(t)\left(S(t) + r'_e - r'_g\right), \tag{1.35}$$

where $P(0) = r'^2_g + r'^2_e$ is the initial state's purity and $r'_i = \dfrac{r_i}{1 - r_m}$ is the population of level $i = g, e$ rescaled by the population of level $|m\rangle$. Notice that, since the adiabatic elimination condition ensures that the population of level $|m\rangle$ is unchanged, higher temperatures reduce the amount of useful population for the QB and therefore its maximum purity. These results can be checked for three different temperatures in Fig. 1.5.

1.2.6 Charging efficiency

Another figure of merit which is important in the characterization of the charging process of a quantum battery is the charging efficiency. Because the classical power source ω_L is injecting energy in the coupled battery+field system, it is important to characterize how much of that energy is indeed going into the battery and how much is leaking to the

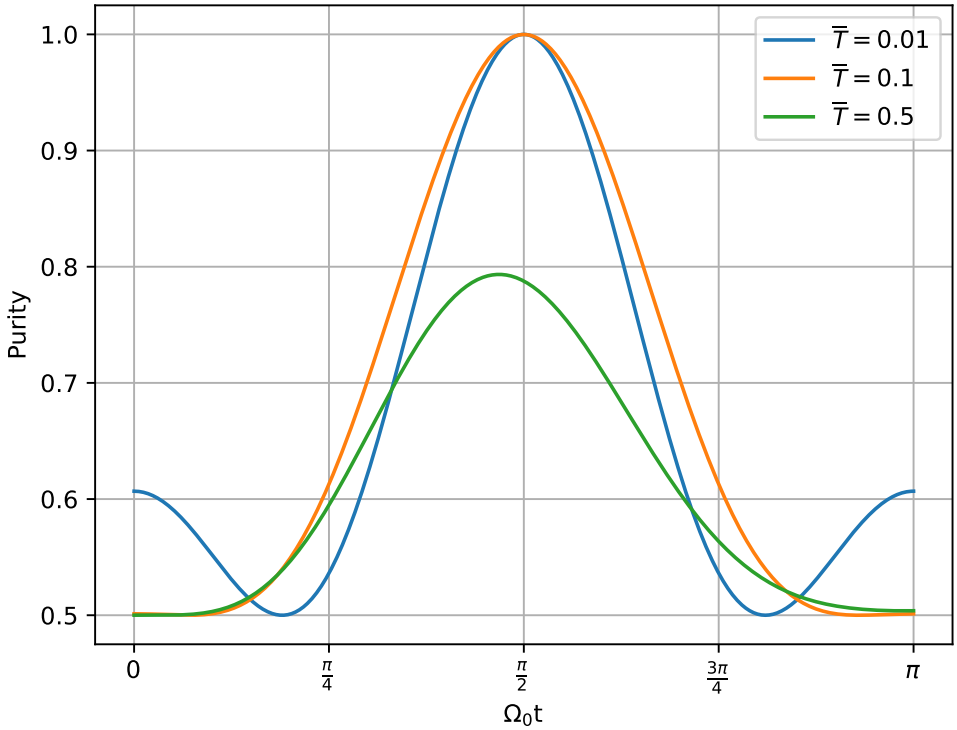

Figure 1.5: For low but non-vanishing temperature, the purity of the effective two-level system used as quantum battery is shown to achieve unit in the non-selective regime of this charging protocol. The time of maximum purity coincide with the optimization time for better storage of ergotropy in the battery. Here, Ω_0 is the effective Rabi frequency of the lowest energy doublet.

charger. To define that, we recall the main demand of a quantum battery which is to have its energy extracted on demand. This means that the total amount of energy absorbed by the battery which should be considered, in this case, is the ergotropy $\mathcal{E}^q_{QB}$ itself, as given by equation (1.29).

$$\mathcal{E}^q_{QB} = 2\Delta U^q_{QB} - \Delta U^c_{QB}. \tag{1.36}$$

On the other hand, the total injected energy can be computed by a simple analysis of the conservation of energy in the global system:

$$W_L = \Delta U^q_{QB} + \Delta U^q_{ch}, \tag{1.37}$$

where ΔU^q_{ch} is the variation of internal energy of the quantum EM field used as charger. This can be computed at any arbitrary time of evolution directly from the traced state of the charger field, which is given by

$$\rho_{ch}(t) = \rho_{ch}(0) + \sum_{n=0}^{\infty} S_n(t) \left(|n+1\rangle\langle n+1| - |n\rangle\langle n| \right). \tag{1.38}$$

This furnishes

$$\Delta U^q_{ch}(t) = \mathrm{Tr}\left(\hbar\omega_q \hat{a}^\dagger \hat{a} \left[\rho_{ch}(t) - \rho_{ch}(0) \right] \right) = \hbar\omega_q S(t), \tag{1.39}$$

in a similar expression as for the battery's energy variation (1.28). Gathering these results we find that the total energy injected by the classical power source is

$$W_L(t) = (\hbar\omega_{eg} + \hbar\omega_q) S(t). \tag{1.40}$$

At the numerically found time τ_q which optimizes the energy input into the battery, we can therefore write

$$W_L(\tau_q) = \frac{\omega_q + \omega_{eg}}{\omega_{eg}} \Delta U^q_{QB}(\tau_q), \tag{1.41}$$

and the charging efficiency η is defined as

$$\eta \equiv \frac{\mathcal{E}^q_{QB}(\tau_q)}{W_L(\tau_q)} = \left(\frac{\omega_{eg}}{\omega_q + \omega_{eg}} \right) \left(\frac{2\Delta U^q_{QB} - \Delta U^c_{QB}}{\Delta U^q_{QB}} \right). \tag{1.42}$$

This expression can be rewritten in terms of the classical-to-quantum relative energy gain K_q and the parameter $\xi = \omega_q/\omega_{eg}$ as

$$\eta = \left(\frac{1}{1+\xi} \right) \left(1 + \frac{K_q}{1+K_q} \right), \tag{1.43}$$

where $\xi > 1$ is intended in order to achieve the desired quantum advantage over the fully classical protocol. Notice that, as previously discussed, the enhancement in K_q due to the

vacuum of the quantum field gets larger as ξ increases. This reasoning, together with the expression (1.43) for the charging efficiency leads to the conclusion that the maximum energy gains are achieved at lower efficiencies. Indeed, it can be straightforwardly checked that, for a fixed value $\xi \gg 1$ we have $K_q \gg 1$ and the maximum efficiency achievable is

$$\eta_{max} \approx \frac{2}{\xi}. \tag{1.44}$$

This can also be contemplated in figure 1.6, where it becomes clear that there is always an ideal value of ξ if one wishes to achieve the highest energetic gain at the best efficiency possible.

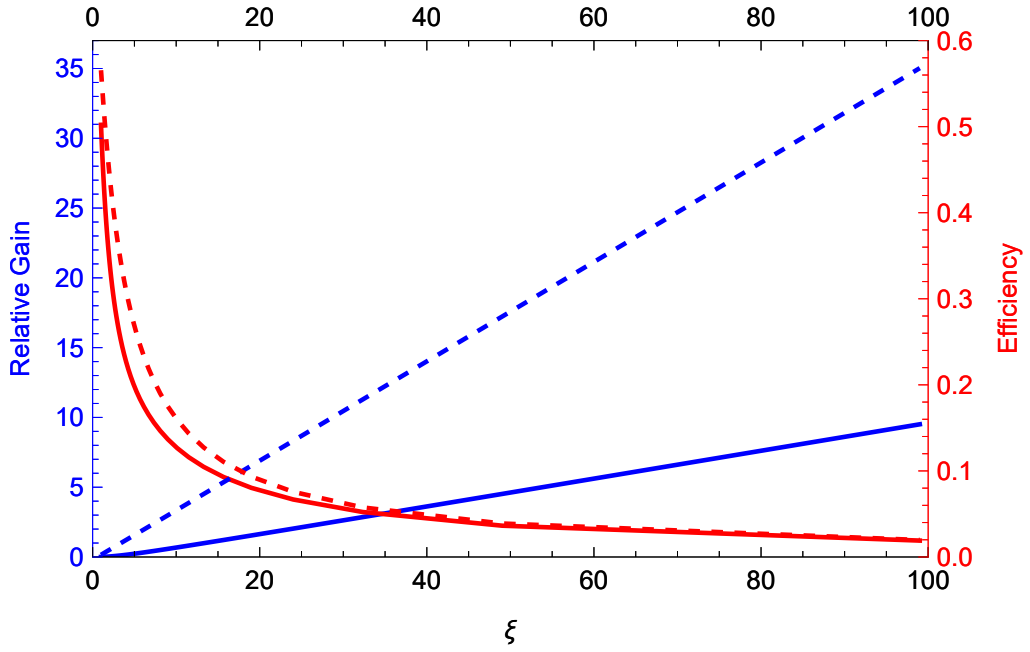

Figure 1.6: Relative gain K_q and efficiency η as functions of the parameter $\xi = \omega_q/\omega_{eg}$ for different values of the dimensionless temperature $\overline{T} = k_B T/\hbar\omega_m$. In here, $\overline{T} \approx 0.1$ for the solid lines and ≈ 0.4 for the dashed lines. Furthermore, we set $\frac{\Delta}{2\pi} = 1$ MHz, $g = \frac{\Delta}{600}$ and $\Omega_L = \frac{\Delta}{20}$.

1.2.7 Dissipation

So far, all charging regimes were considered in the iso-entropic approximation, where the full dynamics is unitary and no dissipation due to contact with the environment occurs. However, neither the atom nor the quantized field are ever fully isolated from their environment and there will always be heat exchanged with the external reservoir. It is natural to wonder whether the advantage of this protocol still holds under looser assumptions, as well as what its limitations are.

From the atomic perspective, if both $|g\rangle \to |m\rangle$ and $|e\rangle \to |m\rangle$ transitions are dipole coupled, levels $|g\rangle$ and $|e\rangle$ must be of the same parity and, therefore, cannot be dipole coupled themselves. That means that the time scale for direct energy exchange between them is usually much slower than any other time scale of the problem and, in general, the corresponding heat channel can be ignored. Considering the standard Markovian approximation to thermal reservoirs, the overall dynamics of the system is, then, governed by a master equation of the form

$$\dot{\rho}(t) = -i[\hat{H}_{qu}, \rho] + \mathcal{D}[\rho], \tag{1.45}$$

where $\hat{H}_{qu}$ is the full Hamiltonian given by (1.15) and $\mathcal{D}[\rho] = \sum_\mu \Gamma_\mu \left(\hat{L}_\mu \rho \hat{L}_\mu^\dagger - \frac{1}{2}\{\hat{L}_\mu^\dagger \hat{L}_\mu, \rho\} \right)$ is the dissipator superoperator. Here, we have $\mu = gm, mg, em, me, +, -$ ranging over all the heat channels coupled to a heat reservoir. The rates of the non-unitary parts are given by $\Gamma_{jm} = \gamma_{0j}(\overline{n}_j + 1)$, $\Gamma_{mj} = \gamma_{0j}\overline{n}_j$, $\Gamma_- = \gamma_{0q}(\overline{n}_q + 1)$, and $\Gamma_+ = \gamma_{0q}\overline{n}_q$. Here, the γ_0's indicate the spontaneous decay rates and $\overline{n}$'s the average number of photons of the thermal reservoir at frequencies ω_{mj} and ω_q. The respective jump operators are $\hat{L}_{jk} = \hat{\sigma}_{jk}$, $\hat{L}_- = \hat{a}$ and $\hat{L}_+ = \hat{a}^\dagger$.

The couplings to the thermal reservoirs establish at least four typical regimes to the problem, depending on their strength. The first one has already been addressed and corresponds to the situation when γ_0's are much smaller than the effective coupling $\frac{g\Omega_L}{\Delta}$

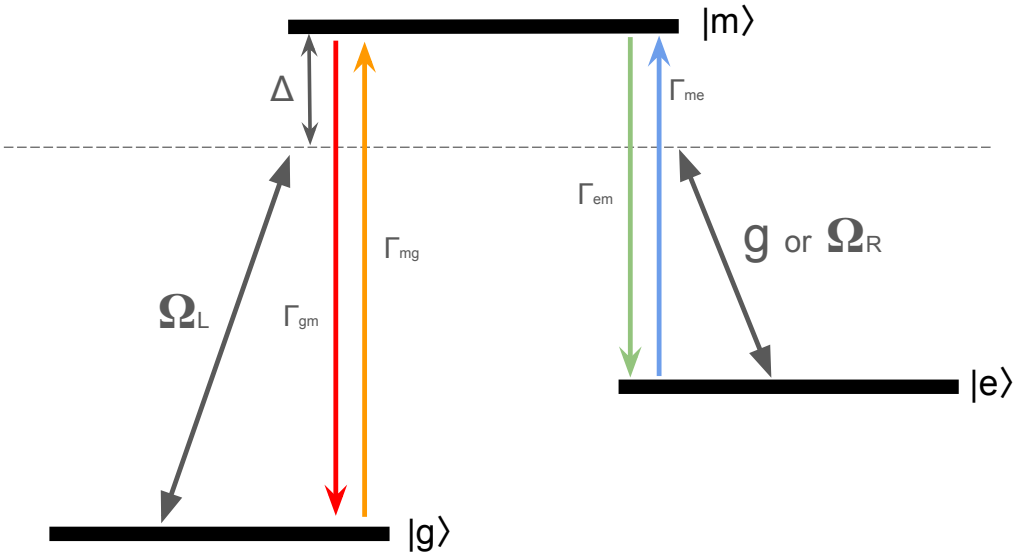

Figure 1.7: The presence of dissipation in the model alters the whole dynamics by including dissipative rates that couple the atomic transitions to the spectra of a thermal reservoir with a fixed temperature. Likewise, the quantum field used as charger is also coupled to a thermal reservoir at the same temperature, with dissipation rates Γ_+ and Γ_- defined in the text.

and the thermal energy $k_B T$ is small compared to the energy gaps of the qutrit $E_{jk} = \hbar\omega_{jk}$. In this case, we can approximate the dynamics by the unitary evolution considered in the previous subsections. We saw in the iso-entropic case that the higher the temperature, the more advantageous the quantum protocol is. This may not hold true when we take into consideration the heat exchanged with the reservoir. As the spontaneous decay rates increase, a combination of effects begin to affect the charging of the battery and may even create optimal temperatures for operation of the protocol. For example, larger values of γ_0 induce decoherence on the quantum field, spoiling the interference that is essential to build up the Rabi flips. It also accelerates the growth of the heat exchange rates Γ's with the temperature.

Differently from the unitary global evolution, the protocol considering dissipation does not have an exact analytic solution. Therefore, we numerically solve the full dynamics (1.45) with no approximations, and compute the relative energetic gain as a function of

the dimensionless temperature $\overline{T}$, which remains a good energetic scale for the system. In figure 1.8 we present K_q as a function of the dimensionless temperature $\overline{T} = \frac{k_B T}{\hbar\omega_m}$ for different values of γ_0. This scale of temperature is relevant to the problem because it regulates the population of level $|m\rangle$. Although each reservoir has its own spontaneous decay rate, they all produce similar effects on both K_q and η, therefore we have considered a single γ_0 for all of them. The result was obtained by solving the full dynamics of the open quantum system, *i.e.*, the master equation (1.45) with the complete Hamiltonian, and choosing the best τ_q for each temperature. In these plots, $\frac{\omega_m}{2\pi} = 10^{12}$ Hz, $\Delta = 2\pi$ MHz $= 600g = 20\Omega_L$, $\xi = 99$, $r = 1/30$.

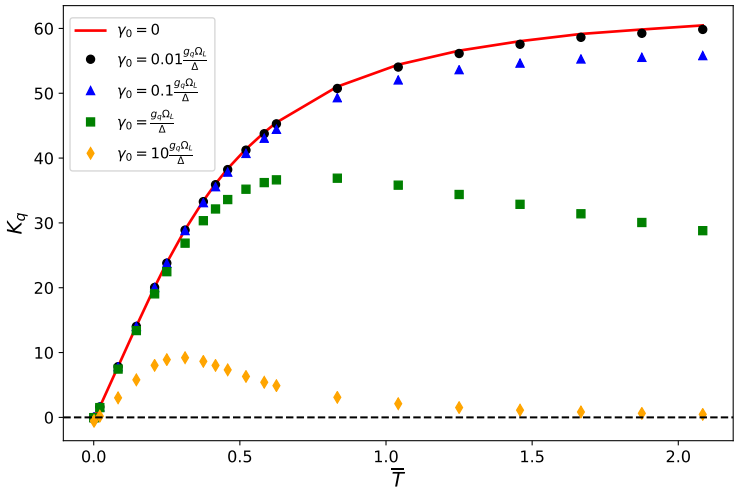

Figure 1.8: Relative gain as a function of the dimensionless temperature $\overline{T}$ for different values of spontaneous decay rates γ_0 and for $\xi = 99$, $\frac{\Delta}{2\pi} = 1$ MHz, $g = \frac{\Delta}{600}$, $\Omega_L = \frac{\Delta}{20}$. The solid curve is obtained from the global unitary evolution with $\hat{H}_{QB}$. The dotted curves are numerical solutions of the open system dynamics with full Hamiltonian.

As previously discussed, for $\gamma_0 \ll \frac{g\Omega_L}{\Delta}$ we reach the unitary regime calculated with Hamiltonian (1.18) (solid curve), except for very high temperature ($\overline{T} \approx 2$) when the population of level $|m\rangle$ becomes too significant and start to affect the protocol as a whole. As we increase γ_0, effects such as decoherence of the quantum field and the augmented relaxation rates Γ_μ begin to limit the quantum advantage. These effects become particularly relevant when the Γ's rates approach the effective battery-charger

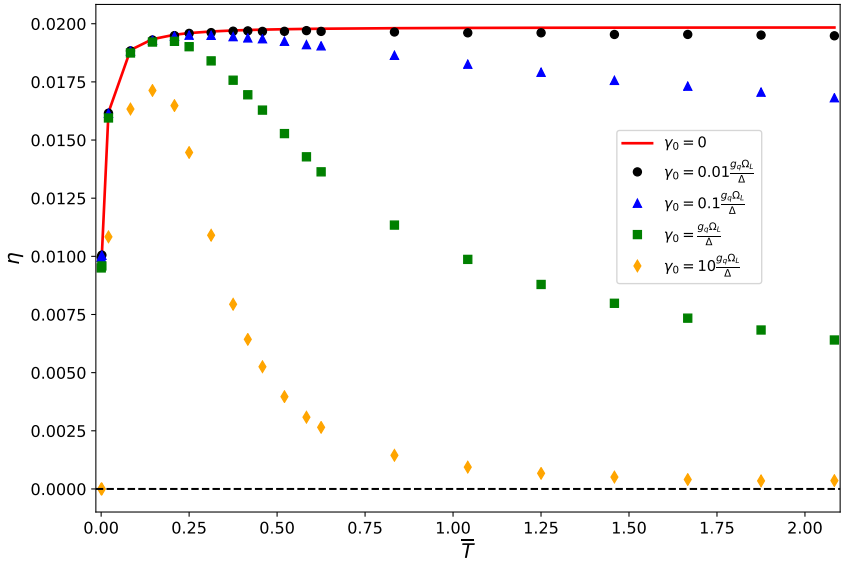

Figure 1.9: Efficiency as a function of the dimensionless temperature $\overline{T}$ for different values of spontaneous decay rates γ_0 (same parameters). The dotted curves are numerical solutions of the open system dynamics with full Hamiltonian.

coupling $g\Omega_L/\Delta$. Note, however, that even for such values of dissipation the quantum protocol can still produce gains 30 times larger than its classical counterpart for $\xi = 99$. Finally, a fourth effect takes place for higher values of γ_0 and at much higher temperatures: when Γ's become of the order of Δ the heat exchange eventually brings the transition back into resonance, in which case level $|m\rangle$ cannot be adiabatically eliminated any more and the charging scheme breaks down.

In figure 1.9 we repeat the numerical calculations of the open system dynamics (same parameters), this time for the efficiency. Again, we see that very low γ_0's are consistent with the iso-entropic hypothesis, whereas higher values of the spontaneous decay rates severely affect the efficiency, specially for higher values of $\overline{T}$. Note that for some parameters, the plotted efficiency is corrected to $\eta = \frac{\mathcal{E}^q_{at}}{W_L + Q_{em}}$ to adjust for the fact that the $|e\rangle \to |m\rangle$ reservoir may also inject energy in the system in the form of heat Q_{em}. The correction takes place whenever we obtain $Q_{em} > 0$.

1.3 Overview

Despite its simplicity, the selective regime of operation derived in the previous section was shown to be completely effective in fully charging the battery whenever one is able to experimentally perform the necessary sequence of detunings. Even though such full charge is only achieved in the asymptotic limit, which most of the times is not straightforward for implementation, it can be checked that just a few detuning steps is already enough to have a good amount of ergotropy stored in the atomic battery.

Moreover, when time of operation is a valuable resource (as it is in most of the cases), we have also seen that the single-shot scenario of operation is also effective in providing ergotropy to the quantum battery, even though, in this case, it is the non-selective regime which is most efficient. We have analysed all possible scenarios, both selective and non-selective regimes, for a wide range of parameters in order to fully characterize these results. More than that, we have also explored the grounds where dissipation plays its role in both the battery and charger, by analysing our protocol under the Markovian approximation for the interaction between the relevant systems and a thermal bath playing the role of environment.

In order to complete our analysis, we turn back to the iso-entropic protocol. More specifically, we retrieve our result that the relative energetic gain K_q gets bigger as the charger/battery gap ratio ξ increases. It means that, for a fixed atomic gap ω_{eg}, the charger's gap size ω_q has a direct influence on how much energy is injected from the power source into the battery. Conversely, larger ξ also means that the efficiency of charging drops, which leads to the conclusion that although a large amount of energy is going into the battery as ergotropy, an even larger amount is going into the quantum field. Notice that, so far, we have considered the quantum field solely as an autonomous charger which exploits, through the selective interaction, the presence of its vacuum in order to boost the battery charging. However, our derived results for K_q and η have provided the

interpretation that the quantum field itself benefits even better from our protocol. It is left for investigation, then, what is the role played by the cavity field in this setup, and if it is possible to explore the atom+field interaction in order to achieve additional gains for the latter.

As a final remark, we call the attention for the fact that in a general protocol where an atom interacts with a quantum field, the presence of the vacuum tends to create deleterious effects as far as charging the atom is regarded. The reason for that is notorious and easy to understand: the no-photon state in general acts as a sink of excitations, which is unhelpful if one wishes to provide the atomic quantum battery with energy. The fact that this protocol indeed thrives on the presence of the vacuum shows the real quantum advantage of employing it for charging a quantum battery.

Chapter 2

Collectively charging quantum batteries

At the end of the previous chapter we have discussed how an anti-Jaynes-Cummings configuration can be harnessed to fully charge an atomic quantum battery. Parallel to that, we concluded that for a single-shot scenario the non-selective regime of operation is the one responsible for achieving the better charge possible. Surprisingly, the energetic gain (relative to the fully classical protocol) could be enhanced by increasing the charger/battery gap ratio, but to the expense of lowering the charging efficiency. As we concluded, this meant that even though the atomic battery was being better charged, most of the power coming from the classical source was actually being transferred to the charger. In this chapter, we investigate if the quantum electromagnetic field can also be thought of as a battery which is mutually charged with the atom, and what the effects of extra quantum resources in this protocol are. More specifically, we tackle on eventual correlations that can be previously present in a chain of atomic batteries which sequentially interact with the quantum field.

2.1 Hybrid quantum batteries

(*Phys. Rev. A 108, 052218*)

On a novel approach, following the main results found previously, we consider the

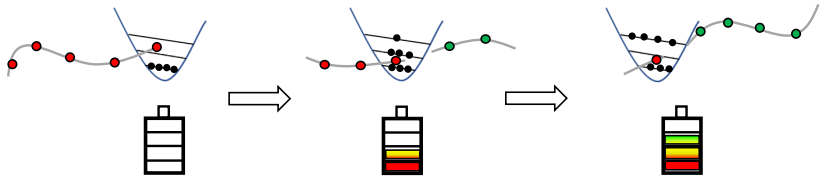

Figure 2.1: A hybrid battery formed by a moving (atoms) and standing still (quantum field) components is powered by classical light. The $k-th$ atom's flying time in the cavity is designed to last the necessary amount of time $\Delta\tau_k$ such that both batteries are maximally charged in the non-selective regime.

whole system atom + field as a hybrid quantum battery, *i.e.*, a global system composed of separate degrees of freedom which are mutually charged by a classical power source. More specifically, we will consider an assembling line of atomic batteries sequentially colliding with a single-mode quantum field inside a cavity. The flying time is individually adjusted in order to optimize the energetic charge of both the atom and quantum field QBs, which are engineered to work on the non-selective regime. We choose so since, as we saw in the previous chapter, this is the regime which mostly transfers energy for a single-shot, time-limited, injection of energy. The basic setup of our toy model is shown in Fig. 2.1.

Each collision is described by an anti-Jaynes-Cummings interaction given by the effective Hamiltonian

$$\hat{H}_{eff} = -\frac{g^2 N}{\Delta}\hat{\sigma}_{gg} - \frac{g^2\hat{a}^\dagger\hat{a}}{\Delta}\hat{\sigma}_{ee} - \frac{g\Omega_L}{\Delta}\left(\hat{\sigma}_{ge}\hat{a} + \hat{\sigma}_{eg}\hat{a}^\dagger\right). \tag{2.1}$$

Again, g (Ω_L) is the coupling to the quantum (classical) field ω_q (ω_L), Δ is the off-resonance detuning $\Delta = \omega_{mg} - \omega_L = \omega_{me} - \omega_q$, and level $|m\rangle$ is adiabatically eliminated from the dynamics in each atom. Furthermore, N is a positive natural number applied by a d.c. Stark shift correction to the energy of level $|g\rangle$.

As the evolution of each atom has already been discussed in the previous chapter, we now focus on the progress of charging the whole chain and the quantum field. In our

collisional model of non-interacting atoms, the individual state of each atom in the chain, before the interaction with the field, is thermal, and we compare three different scenarios for the global state of the atomic chain: a) it is uncorrelated; b) it presents classical correlation; and c) it is an entangled state. In every case, each atom of the chain evolves unitarily with the quantum field under the effective Hamiltonian $\hat{H}_{eff}$ for a time $\Delta\tau_k$, where k represents the interaction with the k^{th} atom of the chain. Our goal is, naturally, to characterize the presence of classical and quantum correlations in the global state of the chain as possible resources to enhance the charging performance.

2.2 Uncorrelated atomic chain

In the first scenario, we design the assembling line with K atoms such that its global state is given by

$$\rho_{atom}^{chain}(\tau_0) = \rho_{atom}^{(1)} \otimes \rho_{atom}^{(2)} \otimes \cdots \otimes \rho_{atom}^{(K)}, \tag{2.2}$$

where each atom's individual state, as well as the quantum field's initial state, is given by a Gibbs distribution

$$\rho_j = \frac{e^{-\hat{H}_j/k_BT}}{Z}, \tag{2.3}$$

where $Z = \mathrm{Tr}\, e^{-\hat{H}_0^j/k_BT}$ $(j = atom, field)$, $\hat{H}_0^{atom} = \sum_{i=g,e,m} \omega_i |i\rangle\langle i|$ and $\hat{H}_0^{field} = \omega_q \hat{a}^\dagger \hat{a}$.

At each collision, a single atom of the assembling line interacts with the E.M. field for a finite time interval $\Delta\tau_k = \tau_k - \tau_{k-1}$, and energy is injected in both systems by the external power source. After the $k-th$ interaction, the energies gained by the interacting atom and by the E.M. field are respectively given by

$$\Delta U_k^{atom} = \hbar\omega_{eg} S(\tau_k), \tag{2.4}$$

$$\Delta U_k^{field} = \hbar\omega_q S(\tau_k), \tag{2.5}$$

where $U_k^j = \mathrm{Tr}\left(\rho_k^j \hat{H}_0^j\right)$ and

$$S(\tau_k) = \sum_{n=0}^{\infty} \delta_n^2 \left[p_g^T p_n(\tau_{k-1}) - p_e^T p_{n+1}(\tau_{k-1})\right] \sin^2\left(\Omega_n \Delta\tau_k\right). \tag{2.6}$$

Here $\delta_n^2 \equiv \dfrac{1}{1+\frac{r^2(n+1-N)^2}{4(n+1)}}$, $\Omega_n = \dfrac{g\Omega_L}{\Delta}\sqrt{\frac{r^2}{4}(n+1-N)^2+n+1}$ is the Rabi frequency of oscillation for the doublet $\{|g,n\rangle, |e,n+1\rangle\}$, with $r = \frac{g}{\Omega_L}$ the selectivity parameter, $p_n(\tau_k)$ is the field's population after the k^{th} collision, and $p_g^T = e^{-\beta\hbar\omega_g}/Z_{atom}$, $p_e^T = e^{-\beta\hbar\omega_e}/Z_{atom}$ are the atomic's initial population which are thermal by construction. In the non-selective limit $r \ll 1$ the dynamics is given by a standard anti-J.C. interaction, where all the doublets take part in the unitary evolution and the exact value of N becomes irrelevant for the dynamics since both δ_n^2 and the Rabi frequency Ω_n in each doublet become independent of N.

The time interval for each collision $\Delta\tau_k$ is chosen in such a way that the energy gained after each interaction is maximized, *i.e.*, the function $S(\tau_k)$ reaches its maximum value in each collision. This maximization must be performed numerically, since all the doublets take part in the dynamics in the desired regime of operation. Furthermore, $\Delta\tau_k$ changes as the E.M. mode charges and higher n doublets become more relevant. Finally note that, since charging only occurs during the interaction with each individual atom, maximizing the total charging of the batteries or the power efficiency of the protocol is equivalent.

Naturally, as the k^{th} interaction occurs, the quantum field's state changes depending on its previous state after interaction with the $(k-1)^{th}$ atom. We are then led to question whether this converges to some asymptotic state. Even more interestingly, in the quantum battery's perspective, is to ask: is there any convergence regarding the internal energy of the quantum field battery?

It turns out that, for an assembling atomic line initially on state (2.2), the answer is

yes. In Fig. 2.2 we display the field's internal energy variation $\Delta U_k^{field} = U_{k+1}^{field} - U_k^{field}$ per collision for different values of the initial state's temperature. In here, both quantities are rescaled by $\hbar\omega_m$, the highest energy value of the whole system.

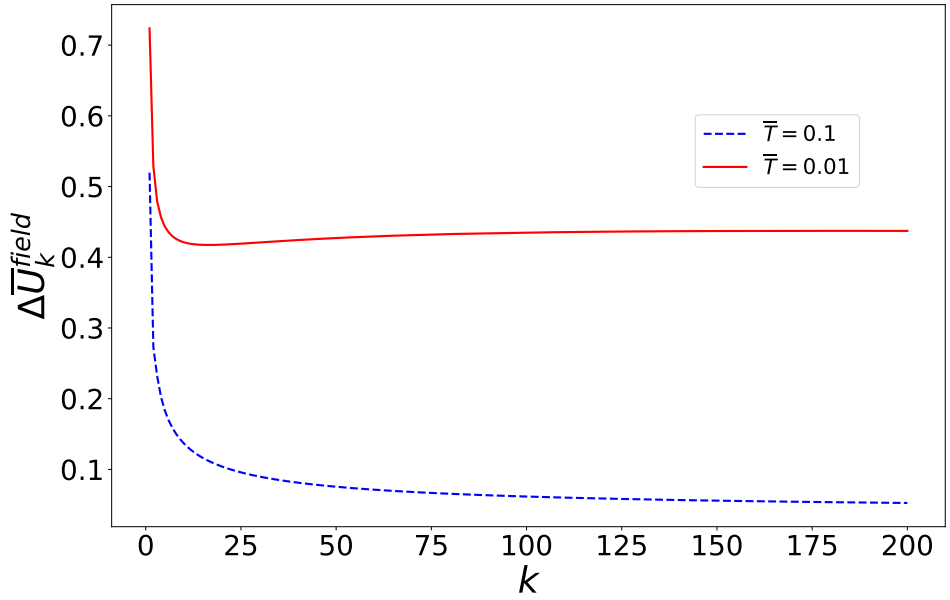

Figure 2.2: Plot of the E.M. energy gained per collision for two different temperatures. Here $\overline{U} = U/\hbar\omega_m$ and $\overline{T} = k_B T/\hbar\omega_m$ are the dimensionless energy variation and temperature. The parameters used for this plot are $\omega_q = 0.99\omega_m$, $\Omega_L/g = 30$, $\Delta/2\pi = 1$ MHz, $g = \Delta/600$ and $\omega_m/2\pi = 10^{12}$ Hz.

As we see in Eqs. (2.4) and (2.5), this behaviour is similar for both atom chain and field. Notice that the protocol works better for lower temperatures, *i.e.*, the energy gain increases when the temperature decreases. This can be physically explained by the fact that for lower temperatures the excitations are predominantly distributed over the lowest lying energy levels and, therefore, population inversion in each collision is larger, which renders more accumulated energy gain. We also see that the energy gain per collision converges to a finite asymptotic value greater than zero. This can be understood by verifying that the charging process for the stationary battery slowly drags it into an asymptotic distribution. The high degree of disorder of the initial state of the uncorrelated chain is responsible for raising the populations of different levels of the E.M. field's state

at each collision. More than that, the fact that every collision is similar and independent ends up generating a Poisson distribution in the E.M. field as can be checked in Fig. 2.3.

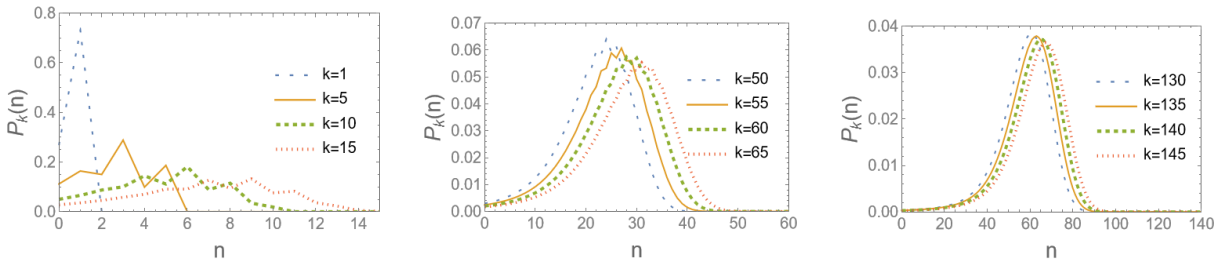

(a) (b) (c)

Figure 2.3: Initial (a), intermediate (b) and asymptotic (c) states for the quantum field after k collisions. These plots are performed for the dimensionless temperature $\overline{T} = 0.01$ for the case of uncorrelated atomic chain.

Initially in a thermal state, the field starts to spread as the first atoms in the chain excites higher doublets. Since the global chain state is fully uncorrelated, this degree of disorder is partially passed to the field, which absorbs part of this entropy and starts to build a spread distribution over increasing average number of photons.

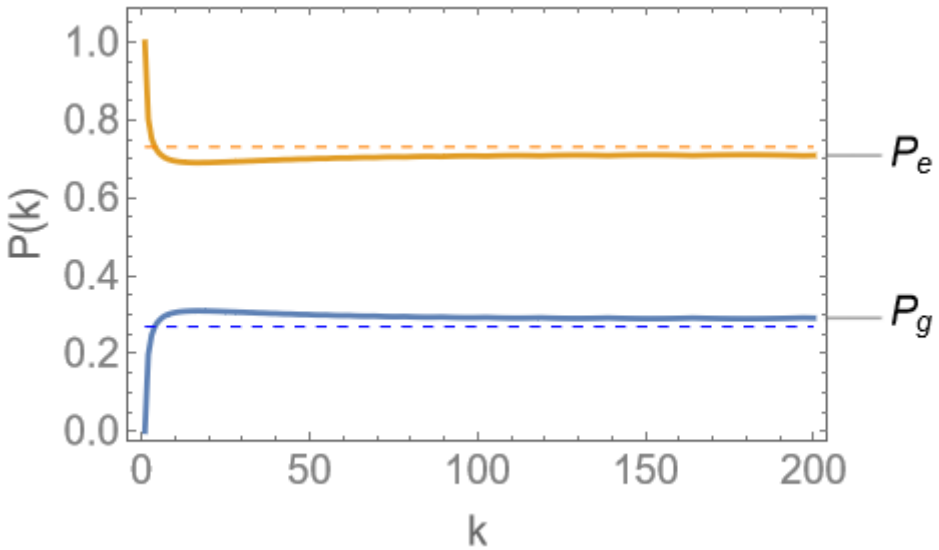

Figure 2.4: The dashed lines represent the Rabi population inversion when an atom interacts with a classical field. The asymptotic behaviour of the field into a coherent state induces an also asymptotic behaviour in the final state's populations of each atom after interaction with quantum field.

After a certain number of collisions (which is highly dependant on the initial state's

temperature) it asymptotically achieves a large coherent state which, for the purpose of the atomic dynamics, works as a classical field. This means that, after enough collisions with uncorrelated atoms, all the following collisions just implement Rabi flips in the atoms and slightly displace the E.M. field. This asymptotic behaviour to the classical nature can be seen in Fig. 2.4, in which the k^{th} atomic population is plotted after the collision has happened.

This semi-classical behaviour is specifically due to the uncorrelated nature of the atomic chain's global state and is not present when correlations are introduced in the global state of the system, as we see next.

2.3 Initial correlations in the atomic chain

In the previous section we have derived general results for the hybrid charging scheme when the battery chain is composed by non-interacting, uncorrelated atoms initially in a thermal state. Since each interaction with the quantum field is unitary, there is no locally-produced entropy, and the k^{th} atom + field reduced state has the same degree of purity before and after charging. However, we may still investigate the role of global correlations in the overall protocol. We do so by designing atomic chain's states which are locally equivalent to the previous scenario, but possess quantum or classical correlations between each atom, and we compare whether there is any advantage arising from these features.

2.3.1 Classically correlated and entangled states

The two states we are interested in investigating in this section are given by

$$\rho_{atom}^{C.C}(0) = p_g^T |gg...\rangle\langle gg...| + p_e^T |ee...\rangle\langle ee...|, \tag{2.7}$$

$$|\psi_{atom}(0)\rangle = \sqrt{p_g^T}\,|ggg...\rangle + \sqrt{p_e^T}\,|eee...\rangle\,. \tag{2.8}$$

The first state (2.7) describes a classically correlated (C.C) streamline of atoms where, if one is found for instance in the ground state with probability p_g^T, so are all other atoms. Parallel to that, the GHZ-like pure state (2.8) describes a global state of entangled atoms in the chain. While the correlations present in the former one are of classical nature, the presence of coherence in the latter makes it completely different in nature.

In both cases, however, the coefficients $\{p_g^T, p_e^T\}$ are chosen such that each individual atom is in the same thermal state as before, which allows us to compare what are the impacts solely of the presence of classical and quantum correlations in the hybrid charging. The initial state of the hybrid battery (atomic chain + field) will be given by $\rho(0) = \rho_{atom}^{j}(0) \otimes \rho_{field}(0)$, where $\rho_{field}(0)$ is given by (2.3) and ρ_{atom}^{j} is either $\rho_{atom}^{C.C}$ or $|\psi_{atom}(0)\rangle \langle\psi_{atom}(0)|$.

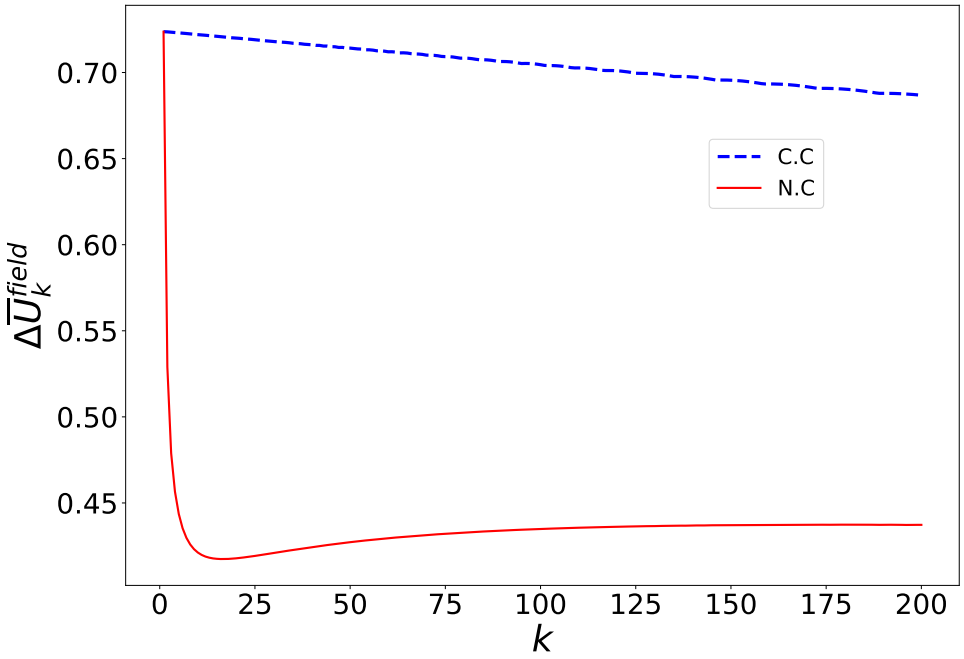

Figure 2.5: Energy gain per collision for the E.M. field considering two different initial states for the atoms in the assembling line: a classically correlated state (C.C) and an uncorrelated state (N.C). Parameters are all the same as before, and $\overline{T} = 0.01$.

To show how the presence of correlations in the initial state of the atomic system

affects the performance of the charging protocol, we plot in Fig. 2.5 the field's energy gain per collision in both cases when the atoms are uncorrelated (N.C), and when the atoms are initially in the C.C state. As in the previous section, the energy gained in each stroke by the colliding atom and the field is still determined by the same expression (2.6) and the overall split of the gained energy between the atom and the E.M. field still depends on the the ratio ω_{eg}/ω_q.

It is clear from Fig. 2.5 that the correlation between the atoms in the streamline increases the energy gain of the E.M. field. This can be understood by the fact that the correlation reinforces the population transfer to higher number states: atoms in the ground state are the ones that allow for the largest overall gain in the anti-J.C. scenario, and the probability of having N sequential atoms in level $|g\rangle$ is p_g^T for the correlated case and $\left(p_g^T\right)^N$ for the uncorrelated one. In fact, the number of ground state atoms for the uncorrelated case follows a binomial distribution of rate p_g^T and the only way for both overall probabilities to coincide is at $T = 0$ ($p_g^T = 1$).

The same result holds for the entangled atomic chain. This is explained by considering a simple example of only two atoms in the chain ($K = 2$) and assuming that the temperature is small enough for the population of the E.M. field to be concentrated in the ground state $|0\rangle$, *i.e.*, $k_B T \ll \hbar\omega_q$. In this scenario, we can easily neglect the field's populations p_n for $n \geq 1$ (without any further impact on the atomic chain's state), so that the total system's initial state is given by

$$|\psi(0)\rangle = \left(\sqrt{p_g^T}\,|gg\rangle + \sqrt{p_e^T}\,|ee\rangle\right) \otimes |0\rangle\,. \tag{2.9}$$

In the first collision, the state $|g0\rangle$ undergoes a Rabi oscillation and, since the protocol is set to maximize the energetic gain, we calibrate the interaction to stop whenever $|g0\rangle \to |e1\rangle$. The first collision takes $|\psi(0)\rangle$ into state $|\psi(\tau_1)\rangle = |e\rangle\left(\sqrt{p_g^T}\,|g\rangle\,|1\rangle + \sqrt{p_e^T}\,|e\rangle\,|0\rangle\right)$ and the second collision takes $|\psi(\tau_1)\rangle$ into $|\psi(\tau_2)\rangle = |ee\rangle\left(\sqrt{p_g^T}\,|2\rangle + \sqrt{p_e^T}\,|0\rangle\right)$. The second atom starts at the partial state $|g1\rangle$ and must undergo a Rabi-flip to $|e2\rangle$. Notice

how, at each stroke, the time window of the protocol is dictated solely by the $|gg\rangle$ part of the initial state, since the presence of the atomic excited state $|ee\rangle$ shields the population of level $|0\rangle$ (the state $|e0\rangle$ is an eigenstate of the effective Hamiltonian (2.1)). All the atoms end up in the excited state, maximizing their charging and the E.M. field ends up on a superposition of the vacuum and a number state equal to the number of collisions.

A similar calculation carried on for the C.C. case generates the E.M. field state

$$\rho_{field}(\tau_2) = p_g^T |2\rangle\langle 2| + p_e^T |0\rangle\langle 0|, \tag{2.10}$$

while also fully charging the atomic chain. Since the energy gained by the E.M. field only depends on the population of each eigenstate of its free Hamiltonian (*i.e.* the coherences that appear in the entangled case do not affect it) both entangled and classically correlated cases are energetically equivalent. That is not to say that both cases are absolutely equivalent, as we see in the following subsection.

2.3.2 Work extraction and ergotropy

As previously mentioned, the presence of coherences in the energy eigenbasis do not directly alter the field's internal energy. However, this is certainly not the case for the ergotropy. It has been previously studied in the literature [54–56] that correlations can be used to boost the performance of a quantum battery, and we have already checked how they impact the energetic transfer in our system. In this subsection we proceed to analyse the stored ergotropy.

Following Eq. (1.5) for the ergotropy of the system, we can calculate it for the field's Hamiltonian $\hat{H} = \hbar\omega_q \hat{N}$, where $\hat{N}$ is the number operator of the field mode ω_q, which has increasing-in-order eigenvalues $E_i = \hbar\omega_q i$:

$$\mathcal{E} = \hbar\omega_q \sum_{i=0}^{\infty} p_i^{dec} \left(\langle p_i^{dec}| \hat{N} |p_i^{dec}\rangle - i \right). \tag{2.11}$$

The field's ergotropy written in this form eases the visualization that the positive contribution to the maximal stored work in the field is due to states with higher mean occupation numbers, and increases as they get more and more populated. Therefore, the shifting of the field's population towards higher mean occupation numbers is directly linked to the stored amount of extractable work: the faster it shifts, the more ergotropy it stores with a given chain size.

Following the same simple reasoning employed in the example discussed at the end of the previous subsection, we may calculate the final state of the field at the same regime of relative low temperatures ($k_BT \ll \hbar\omega_q$). For a chain with K atoms, the final states of the field for the entangled and the classically correlated schemes are, respectively

$$\rho^{EN}_{field}(\tau_K) = p_g^T|K\rangle\langle K| + p_e^T|0\rangle\langle 0| + \sqrt{p_g^T p_e^T}\left(|K\rangle\langle 0| + |0\rangle\langle K|\right), \tag{2.12}$$

$$\rho^{C.C}_{field}(\tau_K) = p_g^T|K\rangle\langle K| + p_e^T|0\rangle\langle 0|. \tag{2.13}$$

As we can see, by comparing these states with the ones depicted in Fig. 2.3, both the latter cases shift the field's mean population faster than the former, uncorrelated case. This shows that the presence of correlations also presents advantages when ergotropy is regarded. We may then wonder whether the nature of these correlations, *i.e.*, whether they are quantum or classical, also affects the said figure of merit.

To do that, we diagonalize the field's state $\rho^{EN}_{field}(\tau_K)$ to find its spectral decomposition and, using the expression (2.11), we find the stored ergotropy in the field for each correlated case as given by

$$\mathcal{E}_{EN} = \frac{K\hbar\omega_q}{1+\frac{p_e^T}{p_g^T}}, \tag{2.14}$$

$$\mathcal{E}_{CC} = \hbar\omega_q(Kp_g^T - p_e^T), \tag{2.15}$$

and their ratio given by

$$\frac{\mathcal{E}_{EN}}{\mathcal{E}_{CC}} = \frac{K}{K - \frac{p_e^T}{p_g^T}} = \frac{K}{K - e^{-\beta\hbar\omega_{eg}}}. \tag{2.16}$$

As we see, this ratio approaches unit, as $\beta \to \infty$, for whatever chain size. Furthermore, even at non-zero, but still low, temperatures, the ergotropic gain ratio diminishes with longer atomic streams. Altogether, these results illustrate that the entangled state has effectively no considerable gain upon a classical correlation between the atoms.

For arbitrary values of the temperature, however, evaluating the ergotropic difference between the two types of correlation is a more involved task. This is so because in this case we can no longer neglect the non-vacuum populations of the field, which implies that more than a single doublet should evolve during each collision, and the optimal time for maximizing the energy extraction must be found numerically. Furthermore, solving the evolution equations for the entangled initial state is a hard computational task, since the total Hilbert space dimension scales exponentially with the number of inputs. For the sake of this investigation and for the reasons just presented, we compare both types of correlations outside of the relative low-temperature regime for a chain size of up to seven atoms. Even at this regime, the main source of additional ergotropy is the quantum coherence present in the entangled state but, as we display in Fig. 2.6, this increment poses no significant gain over the C.C scenario and, from the point of view of resource theory, may not even cover the total entropic cost for creating the initial entangled state. In addition to that, notice that such increment is only available after the final atom interacts with the field, which is expected since only then the information about the entanglement of the whole chain state is furnished.

Since the entangled global state is a pure state, the entropic cost for creating such a resource is maximal among the ones we used in the protocol. For the classically correlated atomic state, on the other hand, the Von Neumann entropy can be shown to be $S(\rho_{CC}) =$

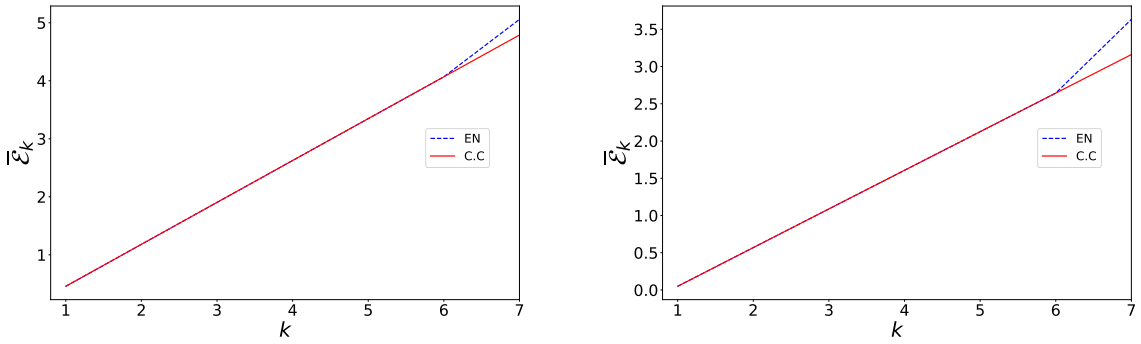

Figure 2.6: Dimensionless ergotropies (normalized by $\hbar\omega_m$) in the field for the entangled and classically correlated initial atomic states, for (a) $\overline{T} = 0.01$ and (b) $\overline{T} = 0.1$. Despite the fact that the entangled initial state increases the amount of ergotropy stored in the field, this increment does not substantially scale with the temperature and may even present losses when the cost for producing such a state is considered.

$\frac{\chi}{\overline{T}}\frac{e^{-\chi/\overline{T}}}{Z} + ln(Z)$, with $\omega_g = 0$, $\omega_e = \chi\omega_m$ and $\overline{T} = \frac{k_B T}{\hbar\omega_m}$ the dimensionless temperature. In order to maintain the population of level $|m\rangle$ under control, to avoid spoiling the adiabatic elimination condition, we should refrain from increasing $\overline{T}$ above a few decimal points. Indeed, in the present case we have limited it to the maximal value of $\overline{T} = 0.1$, which nears the p_m^T population of each atom to be five orders of magnitude lower than p_g^T. This is a safe limit for the operation of the protocol, which also grants us the additional perk of barely neglecting non-vacuum field's populations. This is only true, however, if we work under the assumption of low atomic gap χ.

As one may see from the expression for $S(\rho_{CC})$, the reduced costs with resource are achieved for low values of $\chi/\overline{T}$, and therefore raising the temperature (within the protocol's limits) makes the C.C. initial state a better resource, since we reduce the cost for production and, from Eq. (2.16), the entangled state presents no absolute gain for longer chains. The single scenario where the entangled state may outperform the classically correlated case is for small-sized atomic chains, where the entropic gain for the field in the former setup can be up to twice the amount of work the field stores in the latter.

2.4 Overview

Building up on the previous section, a protocol is proposed where a quantum single-mode of the electromagnetic field is coupled to a stream of atoms with both systems being pumped by an external classical power source in an anti-Jaynes-Cummings configuration. In this protocol both the quantum field and the atomic chain are considered as quantum batteries that are simultaneously charged by the external classical drive and we have focused on studying the role played by correlations in the atomic chain in the performance of the charging protocol. In particular, it was shown that while correlations in the atomic system do not impact the charging dynamics of each individual atom, they do improve the charging of the quantized field by decreasing the total time required to reach a certain level of internal energy. This corresponds to an overall increase in the power efficiency of the charging process when compared to the uncorrelated case. Furthermore, the total amount of stored energy and ergotropy in the field are also higher when correlation is used.

It was also compared the effects of purely quantum (entanglement) versus purely classical correlations. In particular, we have tested the collection of atoms both in a GHZ-like entangled state, with appropriate coefficients to mimic individual atoms in a thermal state, or in its classically correlated equivalent (the equivalent mixture of all atoms up or all atoms down). In this protocol, even though entanglement may generate slightly higher values for the ergotropy of the quantum field, this extra gain certainly does not compensate for the much larger entropic cost to produce GHZ-like states versus their much "cheaper" classically correlated versions. Furthermore, this small extra gain introduced by entanglement becomes less relevant the larger the chain is, vanishing for infinite ones.

Finally, it is worth noticing that further developments of these results may also consider atom-atom interactions within the chain, which could be used to change the correlations

between different pairs of atoms, altogether with their interaction with the mode of the electromagnetic field. In this case, an interesting program would be to analyse how figures of merit such as total charging or the power efficiency of charging the quantum field could be affected by such interactions.

Chapter 3

Environmental charging

Hitherto in this thesis we have investigated charging schemes for single and hybrid quantum batteries which relied solely on one's ability to perform unitary evolutions on the systems of interest. This is specially interesting for quantum batteries that can be realized in regular quantum optics platforms, like the ones we discussed so far (atoms and cavities). In addition to that, we have also partially addressed open system dynamics in the discussion of possible deleterious effects arising in the charging protocols as one's inability to completely control all degrees of freedom which are present in the whole system. This is the case, more specifically, of the natural heat reservoir employed in the numerical treatment of the vacuum-enhanced protocol.

However, even though in that case the presence of an environment was the cause for undesirable behaviour, this is not necessarily true in general grounds. As different studies in the literature suggest [57,58], having total or even partial control over the environmental degrees of freedom can be a valuable resource when the open dynamics is unavoidable. In this chapter, we approach this kind of dynamics in an alternative way: departing from the most general transformations that characterize an arbitrary quantum channel, we derive a Markovian master equation in the Lindblad form that describes the average evolution of a target system which (weakly) interacts with its environment. In addition to that, we explore some symmetry properties of that equation in order to harness potential physical consequences in the overall dynamics.

3.1 General open dynamics

The common framework when open dynamics is regarded is that of two interacting systems: one is our target system, named S, and the other is called environment, named E. In general, E is considered "much larger" than S, in the sense that the former possesses a great deal of degrees of freedom more than the latter. Alternatively, this consideration can be mathematically expressed in the idea that the Hilbert space of E has a much bigger dimension than that of S. However, in here, we do not assume that *a priori*. Instead, both S and E are labels used to encompass a certain amount of different degrees of freedom from some bigger Hilbert space $\mathcal{H}$.

The general approach to the open dynamics [59] considers that one is only interested in the degrees of freedom labelled as S, with E being an unknown or uninteresting set which, however, unavoidably interacts with S, and thus modifies it. In this paradigm, we seek a description for the evolution of S over time, which may be deterministic and continuous, as in the cases given by master equations, or stochastic and intrinsically random. In this section, we quickly derive one such description which departs from two very basic and reasonable assumptions.

The first hypothesis considers that there exists an arbitrary t_0 in which the global system $S + E$ can be unambiguously separated in these two specific sets, *i.e.*, we assume that at such t_0 the global state is given by the product state

$$\rho(t_0) = \rho_S^{t_0} \otimes \rho_E^{t_0}. \tag{3.1}$$

This assumption is fairly reasonable because, in order for S and E to be correlated, they must necessarily interact at some point in their history. In addition to that, since all physical interactions have some limited range, if S and E are initially spatially distant there is always some time t_0 which satisfies this hypothesis. Henceforth, we shall consider $t_0 = 0$ as the initial time for the evolution of S, and the state of this set to be a known

initial state ρ_S^0.

The second hypothesis is that the global system is closed, *i.e.*, the total set of degrees of freedom $S + E$ evolves unitarily in time under a global Hamiltonian[1] H, taken as an Hermitian operator over the Hilbert space of the total system. Since S and E are initially uncorrelated, there exists, at this time, a clear distinction between each set of degrees of freedom and the total Hilbert space can be separated into $\mathcal{H}_S$ and $\mathcal{H}_E$. In this case, both S and E individually evolve unitarily under different Hamiltonians H_0^i ($i = S,\ E$). Once the interaction starts, the total Hilbert space becomes a junction between $\mathcal{H}_S$ and $\mathcal{H}_E$ and the new interaction Hamiltonian, opposed to its individual free counterparts, is defined over the mixed basis of $\mathcal{H}$:

$$H_{SE} = \sum_n \lambda_n \left(S_n \otimes E_n + S_n^\dagger \otimes E_n^\dagger \right), \tag{3.2}$$

where we have made explicit the hermiticity of H_{SE}. Here, λ_n are the *coupling strengths* between S and E, S_n are operators defined over S's degrees of freedom and E_n over E's. Notice that, with no loss of generality, the coupling strengths can always be chosen as real parameters, since any complex phase can be absorbed into the definitions of S_n or E_n. The total Hamiltonian is now given by $H = H_0^S + H_0^E + H_{SE}$, and the global state's evolution is

$$\frac{d\rho}{dt}(t) = -i \left[H, \rho(t) \right]. \tag{3.3}$$

To simplify our treatment, it is convenient to define the interaction picture state $\tilde{\rho}(t) = e^{iH_0 t} \rho(t) e^{iH_0 t}$, with $H_0 = H_0^S + H_0^E$. In this picture, the evolution is given alternatively by

$$\frac{d\tilde{\rho}}{dt}(t) = -i \left[\tilde{H}_{SE}, \tilde{\rho} \right], \tag{3.4}$$

[1]From now on in this chapter we shall stop using the hat symbol for operators, to avoid excessively dense notation.

with $\tilde{H}_{SE} = e^{iH_0 t} H_{SE} e^{-iH_0 t}$ the interaction Hamiltonian in the interaction picture. This Hamiltonian can be explicitly written

$$\tilde{H}_{SE} = \sum_n \lambda_n \left(\tilde{S}_n \otimes \tilde{E}_n + \tilde{S}_n^\dagger \otimes \tilde{E}_n^\dagger \right), \tag{3.5}$$

where we further define $\tilde{S}_n \equiv e^{iH_0^S t} S_n e^{-iH_0^S t}$ and analogously for $\tilde{E}_n$. Notice that, as expected, the change in picture does not alter any of the previous assumptions. Equation (3.4) can be easily solved by

$$\tilde{\rho}(t) = e^{-it\tilde{H}_{SE}} \tilde{\rho}(0) e^{it\tilde{H}_{SE}}, \tag{3.6}$$

where $\tilde{\rho}(0) = \rho(0)$ is given by (3.1). From now we shall work on the interaction picture for all quantities and, for the ease of notation, we drop the *tilde* mark, leaving implied these definitions.

Despite its simplicity in form, Eq. (3.6) encompasses a great deal of information. First, $\rho(t)$ encompasses all the correlations created between S and E at any arbitrary time t. This is to say that any change in E necessarily influences system S and, therefore, alters it. Second, it is not always that these two systems can be distinguishably separated, and any attempt in doing so necessarily implies in loss of information from both S and E. This, as we shall see, introduces corrections to the single dynamics which, nonetheless, are derived from our artificial choice of trying to rule out one system in detriment of the other.

In practical terms, it is not feasible to find an explicit time dependent expression for the global system from (3.6). However, an iterative solution is at hand if we expand the exponential terms for small time steps dt. Recalling that H_{SE} is proportional to coupling constants λ_n, we may truncate the exponential expansion at a time dt such that $\lambda_n dt \ll 1$ for all n. Since the global evolution is continuous, such small times always exist, regardless of the values of λ_n. The first order contribution to the global state is

$$\rho(dt) = \rho_S^0 \otimes \rho_E^0 + \\ - idt \sum_n \lambda_n \left(S_n \rho_S^0 \otimes E_n \rho_E^0 + S_n^\dagger \rho_S^0 \otimes E_n^\dagger \rho_E^0 - \rho_S^0 S_n \otimes \rho_E^0 E_n - \rho_S^0 S_n^\dagger \otimes \rho_E^0 E_n^\dagger \right). \tag{3.7}$$

It turns out that, in most of the applications, this time window is short enough only for correlations, which lie in the joint part of the global Hilbert space, to start building up between S and E. This small dt, therefore, does not provide enough time for the separate parts of the Hilbert space associated to S and E to truly change. A simple example which makes it clear is if we consider E as an harmonic oscillator initially in the fundamental state $|0\rangle\langle 0|$ and $E_n = \hat{a}\delta_{n,1}$ the annihilation operator. For whichever system ρ_S^0 represents, it is very easy to check that, despite some correlation terms are present in $\rho(dt)$, the partial traces over S and E only recover the respective initial states. Of course, this is highly dependent on the initial state, and for some specific cases this first order truncation might be enough to describe the evolution iteratively.

Let us then consider a slightly bigger time interval $d\tau > dt$, such that only $(\lambda_n d\tau)^2 \ll 1$. In this case, we may consider all $d\tau^2$ factors in the exponential expansion. The evolved global state in this case is given by

$$\begin{aligned}
\rho(d\tau) = {} & \rho_S^0 \otimes \rho_E^0 + \\
& - id\tau \sum_n \lambda_n \left(S_n \rho_S^0 \otimes E_n \rho_E^0 + S_n^\dagger \rho_S^0 \otimes E_n^\dagger \rho_E^0 - \rho_S^0 S_n \otimes \rho_E^0 E_n - \rho_S^0 S_n^\dagger \otimes \rho_E^0 E_n^\dagger \right) \\
& + d\tau^2 \sum_{m,n} \lambda_m \lambda_n \left(S_n \rho_S^0 S_m \otimes E_n \rho_E^0 E_m - \frac{1}{2} S_m S_n \rho_S^0 \otimes E_m E_n \rho_E^0 - \frac{1}{2} \rho_S^0 S_m S_n \otimes \rho_E^0 E_m E_n \right) \\
& + d\tau^2 \sum_{m,n} \lambda_m \lambda_n \left(S_n \rho_S^0 S_m^\dagger \otimes E_n \rho_E^0 E_m^\dagger - \frac{1}{2} S_m^\dagger S_n \rho_S^0 \otimes E_m^\dagger E_n \rho_E^0 - \frac{1}{2} \rho_S^0 S_m^\dagger S_n \otimes \rho_E^0 E_m^\dagger E_n \right) \\
& + d\tau^2 \sum_{m,n} \lambda_m \lambda_n \left(S_n^\dagger \rho_S^0 S_m \otimes E_n^\dagger \rho_E^0 E_m - \frac{1}{2} S_m S_n^\dagger \rho_S^0 \otimes E_m E_n^\dagger \rho_E^0 - \frac{1}{2} \rho_S^0 S_m S_n^\dagger \otimes \rho_E^0 E_m E_n^\dagger \right) \\
& + d\tau^2 \sum_{m,n} \lambda_m \lambda_n \left(S_n^\dagger \rho_S^0 S_m^\dagger \otimes E_n^\dagger \rho_E^0 E_m^\dagger - \frac{1}{2} S_m^\dagger S_n^\dagger \rho_S^0 \otimes E_m^\dagger E_n^\dagger \rho_E^0 - \frac{1}{2} \rho_S^0 S_m^\dagger S_n^\dagger \otimes \rho_E^0 E_m^\dagger E_n^\dagger \right).
\end{aligned} \tag{3.8}$$

This second order analytical solution for the global system's state, which is non-linear in the coupling strengths, is very useful in two scenarios: firstly, when the differential equation (3.4) is too cumbersome to be worked out analytically. This is generally the case when the global system has too many degrees of freedom, in which case the state's evolution unravels into a big set of coupled differential equations. Secondly, and most important for the scope of this thesis, when one wishes to achieve an individual evolution for the target system S. In this case, the environmental degrees of freedom are generally thought of as unavoidable parts of the dynamics which therefore guide the evolution of S.

Even though we are mainly interested in the second scenario, let us make a brief digression regarding the first. Whenever the global system presents a highly non-trivial set of differential equations to be solved in order to describe the full dynamics, this second order expansion given by (3.8) can be used as an iterative solution to recover the full dynamics. This can be performed in the following way: given the initial non-entangled state from both S and E, and since S_n and E_n are known for some interaction Hamiltonian, $\rho(d\tau)$ can be calculated to some precision of $\mathcal{O}(d\tau^2)$. From this state, $\rho_S^{d\tau}$ and $\rho_E^{d\tau}$ can be calculated by taking the respective partial traces, and then inserted back in (3.8) to find $\rho(2d\tau)$, and so on. This, after done N times, recovers the full global dynamics at time $t = Nd\tau$. This iteration can be numerically performed in order to calculate the time evolution of any desired observable of the global system. Since these expressions are general, with no assumptions about the nature of the interaction itself (whether strong or weak), this method exactly solves any possible physical evolution when two arbitrary systems interact.

Now let us turn to our main interest, namely the individual evolution of system S. In this case, we must deal with the fact that any attempt to separate S from E necessarily incurs in loss of information about the states of S and E. This loss is irretrievable, in the sense that solely from the evolution of S, one may never reconstruct the exact evolution of the global system. In this paradigm, two alternatives are available: either one considers

E as a direct measuring apparatus of S, in which case the states of E serve as labels to uniquely identify the state of S, or one completely disregards the changes in E, in which case S evolves as an average over all possible outcomes of the changes of E. To illustrate both alternatives, let us study a simple, yet clarifying example.

3.1.1 Example: system in a cavity

For this example, let us consider E as a single mode ω_E of the electromagnetic field inside a cavity. For now, S is still an arbitrary system which can couple to E through an interaction Hamiltonian where $E_n = \delta_{n,1}\hat{a}e^{-i\omega_L t}$. Furthermore, let us say that the latter's initial state is the vacuum $\rho_E^0 = |0\rangle\langle 0|$. In this case, the global system state after $d\tau$ changes to

$$\begin{aligned}\rho(d\tau) = &\left(\rho_S^0 - \frac{1}{2}d\tau^2\lambda_1^2\{S_1S_1^\dagger, \rho_S^0\}\right)\otimes|0\rangle\langle 0| + d\tau^2\lambda_1^2\ S_1^\dagger\rho_S^0 S_1\otimes|1\rangle\langle 1| \\ &- id\tau\lambda_1\left(S_1^\dagger\rho_S^0\otimes|1\rangle\langle 0| - \rho_S^0 S_1\otimes|0\rangle\langle 1|\right) \\ &- \frac{\sqrt{2}}{2}d\tau^2\lambda_1^2\left(S_1^{\dagger 2}\rho_S^0\otimes|2\rangle\langle 0| + \rho_S^0 S_1^2\otimes|0\rangle\langle 2|\right).\end{aligned} \tag{3.9}$$

The first line of this expression represents the changes occurring in the global state which can be separated as changes in S and E individually. The second and third line, in contrast, represent changes that occur in the non-separable part of the Hilbert space. This portion of information is always lost whenever one traces out the degrees of freedom of E.

Let us assume that one wishes to retrieve solely the state of S by following the changes in the state of E. Physically, what one should do is interact E with a third system D, which stands for a detector system that distinguishes among different E states. If D is able to distinguish between the Fock states $|n\rangle\langle n|$, then the outcome of such measurement undoubtedly tells the updated state of S: $\rho_S^{d\tau} \propto \left(\rho_S^0 - \frac{1}{2}d\tau^2\lambda_1^2\{S_1S_1^\dagger, \rho_S^0\}\right)$ if the measurement outcome is $n = 0$, or $\rho_S^{d\tau} \propto d\tau^2\lambda_1^2\ S_1^\dagger\rho_S^0 S_1$ if $n = 1$. The proportionality

factor can be calculated by imposing the normalization of $\rho_S^{d\tau}$. Notice that, in this case, the detector system D stands for any photon-number resolving apparatus as, for instance, a photon-counter. Also notice that, in this case, $n = 0$ means that this detector's needle does not change for a certain amount of small time windows $d\tau$, in which case the state of S has to be continuously updated, until it does and the outcome $n = 1$ implies in a discrete change to ρ_S, associated to a measurement on E being made. This discrete change is called a *quantum jump* [60–63] of the system S, associated to the measurement outcome $n = 1$ made upon E.

Naturally, the detector system D is not unique, as there are many different ways to measure system E's degrees of freedom. Suppose that, somehow, one comes out with a different detection D' which, instead of distinguishing between the Fock basis states, actually probes whether E can be found on states $\hat{P}_\pm = \frac{|0\rangle \pm |K\rangle}{\sqrt{2}}$ for $K = 1$ or $K = 2$. This measurement is described by the set of projective measurements $\{|+\rangle\langle+|, |-\rangle\langle-|, 1 - |+\rangle\langle+| - |-\rangle\langle-|\}$, and the conditional state of the global system is given by

$$\begin{aligned}\rho(d\tau) = &\left(\rho_S^0 - \frac{d\tau^2\lambda_1^2}{2}\{S_1 S_1^\dagger, \rho_S^0\} + \rho_1\delta_{K,1} - \rho_2\delta_{K,2}\right)\frac{|+\rangle\langle+|}{2} \\ &\left(\rho_S^0 - \frac{d\tau^2\lambda_1^2}{2}\{S_1 S_1^\dagger, \rho_S^0\} + \rho_1^*\delta_{K,1} + \rho_2\delta_{K,2}\right)\frac{|-\rangle\langle-|}{2} \\ &d\tau^2\lambda_1^2\ S_1^\dagger\rho_S^0 S_1(1-\delta_{K,1})|1\rangle\langle 1|,\end{aligned} \tag{3.10}$$

where $\rho_1 = d\tau^2\lambda_1^2 S_1^\dagger\rho_S^0 S_1 - id\tau\lambda_1\left(S_1^\dagger\rho_S^0 - \rho_S^0 S_1\right)$ and $\rho_2 = \frac{\sqrt{2}}{2}d\tau^2\lambda_1^2\left(S_1^{\dagger 2}\rho_S^0 + \rho_S^0 S_1^2\right)$. Notice that, if $K = 1$, *i.e.*, the detection is only able to tell the relative phase in the $\{|0\rangle, |1\rangle\}$ subspace, then the updated state of system S is given by $\rho_S^{d\tau} \propto \rho_S^0 - \frac{d\tau^2\lambda_1^2}{2}\{S_1 S_1^\dagger, \rho_S^0\} + \rho_1$ if the outcome is $+1$, or by $\rho_S^{d\tau} \propto \rho_S^0 - \frac{d\tau^2\lambda_1^2}{2}\{S_1 S_1^\dagger, \rho_S^0\} + \rho_1^*$ if the outcome is -1. Notice how, in this case, the final state of system S is astonishingly different from the case of the previous detection apparatus D. Indeed, it now explores the terms present in the previously non-separable part of the Hilbert space, present in ρ_1.

Alternatively, if $K = 2$ in the detection apparatus, *i.e.*, the discriminated relative

phase is now present in the $\{|0\rangle, |2\rangle\}$ subspace, then the updated system state is $\rho_S^{d\tau} \propto \rho_S^0 - \frac{d\tau^2\lambda_1^2}{2}\{S_1 S_1^\dagger, \rho_S^0\} - \rho_2$ if the outcome is $+1$, or $\rho_S^{d\tau} \propto \rho_S^0 - \frac{d\tau^2\lambda_1^2}{2}\{S_1 S_1^\dagger, \rho_S^0\} + \rho_2$ if the outcome is -1, or yet $\rho_S^{d\tau} = d\tau^2\lambda_1^2\ S_1^\dagger \rho_S^0 S_1$ if the detection measures one photon. Notice how, in the latter case, the system's state change upon the measurement outcome $n = 1$ is the same as in the case of detector D measuring in the Fock basis. This illustrates that the change in the state of S when E is being monitored can be extremely dependent on the measuring apparatus D. More specifically, on the set of measurements performed upon E.

Finally, notice that there are infinitely many types of measurements that can be performed on E by different detector systems D, D', D'', etc, each one related to a different change in the state of S. However, for all of them, there is one, invariant, discrimination: the average among all possible outcomes of the measurements performed is always the same. This can be quickly worked out for the case of D and D' described above. If we average over the different outcomes for the measurements made by D and by D', the state of S in both cases change as

$$\rho_S(d\tau) = \rho_S^0 + d\tau^2\lambda_1^2\left(S_1^\dagger \rho_S^0 S_1 - \frac{1}{2}\{S_1 S_1^\dagger, \rho_S^0\}\right). \tag{3.11}$$

Specially, in the case of D', this change does not even depend whether the measurement is probing $K = 1$ or 2. We say that, in the case of this average, the information about the state of E has been erased from the measurement apparatus.

3.2 The averaged evolution

Following the discussion just carried in the aforementioned example, one can naturally raise the question: what is the real evolution of S when no monitoring is performed on E? It turns out that this is a highly non-physical question. To explain why, let us split our reasoning in two different perspectives. Before that, let us assume that the global system

$S + E$ interacts with an even wider system called the universe U, which encompasses the collection of all possible detection systems $\{D, D', D'', ...\}$. In what follows, let us call d_E the amount of degrees of freedom of E, d_S the respective amount for S and $d_U = \aleph - d_E - d_S$ the amount of degrees of freedom of the universe set U. In this case, $\aleph$ stands for a fixed number telling the total amount of degrees of freedom of $S + E + U$.

In the first perspective, E is a "small" environment, in the sense that its amount of degrees of freedom is commensurate with those of S (*i.e.*, $d_E \gtrapprox d_S$). In this case, the total amount of degrees of freedom of U is much bigger than both E's and S's ($d_U \gg d_E, d_S$). In this case, the gross hypothesis of complete isolation between U and E gets even worse, as U encompasses a great amount of detector systems Ds. In this case, the change in S, encoded in the states' labels of E, gets probed by many different detector systems at once, each one in a different measurement basis. In this case, the information about the change in S's state gets redundantly spread across the set of Ds, in which case the net effect is that S only changes as an average of the changes associated to all possible measurements performed over E.

In the second perspective, E is a big environment and $d_E \gg d_S$. As a limiting case, we may even consider E to be the rest of the universe ($d_E = d_U$), in which case there is no external degrees of freedom to represent detectors Ds. For this scenario, it may naively seen that there is absolutely no way that E can be probed for the changes of S, but it is not at all true. This is so because, even when E is a huge environment, it only interacts with S point-wise: the interaction between S and E is *local*, in the sense that only a subset of E interacts with S at each time step $d\tau$. In this case, since E encompasses a great amount of degrees of freedom, it also encompasses their respective interactions, which means that the subsets of E directly interacting with S within $d\tau$ are probed by the rest of the degrees of freedom which do not interact with S at this time. Therefore, the information about the change of S is again redundantly spread across the degrees of freedom of E, meaning that S evolves according to the average of the possible jumps

associated to different measurements over the subset of E that interacts with it.

Both of these perspectives have been adopted to say that, physically, the question of what happens to S whenever E is not being monitored is non-physical: E is always being monitored, be it by external detector systems which are never completely isolated from E, be it by other subsets of E itself (consider for instance the case where E is a big cloud of atoms, but only one interacts with S at a time. The rest of the atoms serve as different probes for measuring the changes of S indirectly). What changes, and this is subtle and crucial, is whether the information, encoded in E, about the respective change of S is *redundantly* measured or not. Whenever this probe is not redundant (for instance, when some single system D can completely probe the changes on S through E) then the evolution of S is given by a series of jumps associated to some measured *pointer* in E (in the example given in the previous subsection, this pointer was given by the outcome of each measurement in the Fock basis by D or by the relative phase in the different subspaces K by D'). On the other hand, when the information about the change in S is redundantly measured, in the sense that it is spread through E and measured by different detectors, than the evolution of the former is averaged among all possible outcomes of the pointers.

These two situations provide two completely different outcomes for the evolution of S, with the first one being a sequence of *stroboscopic* changes, while the second one is a continuous averaged set of changes. Each one, as previously stated, depends whether E's information about S is redundantly spread among D's or not. In the first case, the expression (3.8) tells us everything we need in order to recover the set of jumps happening in S: it suffices to probe E accordingly and the outcome of each measurement tells the updated state of S. In the second case, we can still further simplify (3.8) in order to account for the loss of information about the measurement outcome of E. Averaging (3.8) with all the possible outcomes of measurements made upon E is mathematically equivalent to tracing out all the degrees of freedom of the environment, which leaves us

with the averaged change in S:

$$\begin{aligned}\rho_S^{d\tau} = \rho_S^0 - id\tau \left[\sum_n \lambda_n \,\mathrm{Tr}_E\left(E_n\rho_E^0\right) S_n + \lambda_n \,\mathrm{Tr}_E\left(E_n^\dagger\rho_E^0\right) S_n^\dagger, \rho_S^0\right] \\ + d\tau^2 \sum_{m,n} \lambda_m\lambda_n \,\mathrm{Tr}_E\left(E_m E_n \rho_E^0\right)\left(S_n\rho_S^0 S_m - \frac{1}{2}\{S_m S_n, \rho_S^0\}\right) \\ + d\tau^2 \sum_{m,n} \lambda_m\lambda_n \,\mathrm{Tr}_E\left(E_n^\dagger E_m^\dagger \rho_E^0\right)\left(S_m^\dagger\rho_S^0 S_n^\dagger - \frac{1}{2}\{S_n^\dagger S_m^\dagger, \rho_S^0\}\right) \\ + d\tau^2 \sum_{m,n} \lambda_m\lambda_n \,\mathrm{Tr}_E\left(E_m^\dagger E_n \rho_E^0\right)\left(S_n\rho_S^0 S_m^\dagger - \frac{1}{2}\{S_m^\dagger S_n, \rho_S^0\}\right) \\ + d\tau^2 \sum_{m,n} \lambda_m\lambda_n \,\mathrm{Tr}_E\left(E_m E_n^\dagger \rho_E^0\right)\left(S_n^\dagger\rho_S^0 S_m - \frac{1}{2}\{S_m S_n^\dagger, \rho_S^0\}\right).\end{aligned} \tag{3.12}$$

In equation (3.12) the environmental initial state is only present within the trace numbers that follow the interaction strength. In this case, we may interpret such traces as a change in the effective couplings for the first and second order processes happening inside system S.

At this point, some comments are paramount, and the first one regards the validity of this description. Let us recollect the set of hypothesis made so far:

(1) The smallness of $d\tau$: this hypothesis states that $\lambda_m d\tau$ should be much smaller than unity for all the interaction strengths λ_m;

(2) The initial separability of the global state: initially, every pair of systems S and E can be prepared in a factorized state. However, this separability is in general not kept after the interaction takes place;

(3) Multi-probing of E: in order to associate $\rho_S^{d\tau}$ given in (3.12) to the correct state of the system S at the time $d\tau$, one needs to make sure that all the pointer states of E (each one associated to a different stroboscopic change of S) are measured by detector systems D in a way that all the information about the change of S is redundantly spread.

The attentive reader will immediately point out that, in general, the hypothesis (1) and (3) can not be true at the same time. In order for the environment to be sufficiently probed such that the true state of S is given by (3.12) some multi-measurement time window dt needs to exist. This, most definitely, can play against the smallness of the S-E interaction time $d\tau$. This may or may not be true: for strongly interacting systems, where λ_m is big in some sense, $d\tau$ poses a very narrow time window within which one may very hardly have time to fit the multi-probing hypothesis; on the other hand, both hypothesis are not logically mutually exclusive, since we are still left with the possibility that the multi-probing detector systems may indeed probe E faster than it is able to change due to its interaction with S (if, for instance, the set of D's interact with the relevant pieces of E in a stronger way than the latter interacts with S).

Alternatively, the weak coupling regime is where we comfortably have more space to lay both hypothesis in a definite non-mutually exclusive way. This is so because, since now λ_m's are smaller, the interaction time window $d\tau$ gets loose enough so that it may fit the multi-probing interactions happening within $dt < d\tau$. In this paradigm, we also get as a bonus the fact that, since $d\tau$ is wide enough for the environment to be multi-probed, all the correlations between S and E are wiped out at every time step. This provides the system with the perk that the global state is a factorized state at every step $d\tau$. This, as we shall see in the next section, lets us transform the point-wise map (3.12) into a continuous map for the evolution of ρ_S.

A second comment which automatically comes to the eye by the looks of the map (3.12) is the clear distinction between coherent and incoherent terms. The first order in the time approximation provides a Hamiltonian-like factor $-i[\ \cdot, \rho_S^{d\tau}]$, while the second order provides incoherent contributions to the jump evolution of ρ_S. However, these contributions, in comparison with Eq. (3.8), are only present when the information about S encoded in E's states is erased (for instance, by multi-probing E). This is to say that, despite one may feel tempted to immediately define the summation inside the commutator

as a correction to the Hamiltonian of the system S due to the presence of the environment, this term is only present if the *pointer* states on E carry redundant information about S (*i.e.*, only when E can be averaged out from the dynamics). In other words, whenever one is able to probe the information about S stemming from E's pointer states, this expression cannot be used and we have to stick to the free Hamiltonian as the correct hermitian operator for the internal energy of S. As a conclusion, this term, which is informationally originated, may only be taken as a correction to the system's internal energy for the averaged evolution of S, since it stems from an irretrievable loss of information about E. Whenever the information about E is not lost, the system's internal energy is only correctly measured by its free Hamiltonian H_0^S.

3.3 The Markovian approximation

The collection of hypothesis (1) - (3) laid out in the previous section allows us to make the point-wise map (3.12) into a continuous map for the evolution of S. Particularly, they are always true in the weak coupling regime, when the interaction between S and E takes long enough to happen so that the environmental system can be constantly multi-probed and all the correlations erased at each time step. Mathematically, this can be done by rearranging Eq. (3.12) and then taking the appropriate limit $d\tau \to 0$. However, as we have previously discussed, this limit is non-physical, since we are only able to sustain such a description if the interaction time $d\tau$ is lower limited by the environment's decoherence time dt. Therefore, assuming that $dt \ll d\tau$, we may still perform the derivative approximation for S:

$$\begin{aligned}\frac{d\rho_S}{dt}(t) = \lim_{d\tau\to dt}\ \frac{\rho_S^{t+d\tau}-\rho_S^t}{d\tau} &= -i\sum_n \lambda_n \left[\mathrm{Tr}_E\left(E_n\rho_E(t)\right)S_n + \mathrm{Tr}_E\left(E_n^\dagger\rho_E(t)\right)S_n^\dagger, \rho_S(t)\right] \\ &+ \sum_{m,n}\gamma_m\gamma_n\,\mathrm{Tr}_E\left(E_mE_n\rho_E(t)\right)\left(S_n\rho_S(t)S_m - \frac{1}{2}\{S_mS_n,\rho_S(t)\}\right) \\ &+ \sum_{m,n}\gamma_m\gamma_n\,\mathrm{Tr}_E\left(E_n^\dagger E_m^\dagger\rho_E(t)\right)\left(S_m^\dagger\rho_S(t)S_n^\dagger - \frac{1}{2}\{S_n^\dagger S_m^\dagger,\rho_S(t)\}\right) \\ &+ \sum_{m,n}\gamma_m\gamma_n\,\mathrm{Tr}_E\left(E_m^\dagger E_n\rho_E(t)\right)\left(S_n\rho_S(t)S_m^\dagger - \frac{1}{2}\{S_m^\dagger S_n,\rho_S(t)\}\right) \\ &+ \sum_{m,n}\gamma_m\gamma_n\,\mathrm{Tr}_E\left(E_mE_n^\dagger\rho_E(t)\right)\left(S_n^\dagger\rho_S(t)S_m - \frac{1}{2}\{S_mS_n^\dagger,\rho_S(t)\}\right),\end{aligned} \tag{3.13}$$

where we have defined $\gamma_n \equiv \sqrt{dt}\lambda_n$. This equation for the evolution of system S under the hypothesis made so far actually unravels into an intricate set of d_S^2 coupled differential equations for the elements of the density matrix. Despite its cumbersomeness, the real difficulty to solve such equation arises from the time dependence of the environment state present in the trace corrections to the coupling strengths. Strictly speaking, the environmental evolution could, in principle, be obtained by swapping the letters $E \leftrightarrow S$ in equation (3.12), under the same approximations made to obtain that map. In spite of that, it is generally not possible to take the limit to the continuous as we just did for S, and the reason is that generally E encompasses much more degrees of freedom than S, in a way that the decoherence time within S is much longer than that of E. It is sometimes feasible whenever S and E are commensurate, but in general one needs to stick to the jump evolution to describe E.

One final approximation which can be performed in order to simplify that conundrum is that, due to the difference between the sizes of each subsystem, the state of E changes little to nothing within the time window that S takes to evolve. By this means we can remove the time dependence in the trace numbers and leave the whole set of differential equations in a closed form for $\rho_S(t)$. The set of all the hypothesis made so far is generally

termed the *Born-Markov approximation*, and it describes a great deal of open quantum systems which dwell in this *Markovian* regime. Notice that, in this approximation, the net environmental effect on S is just to modify the rate at which the interaction operators S_n act upon ρ_S, which happens as a function of both the state of the environment and the interaction operators E_n that act upon it. For some combinations of environment state and interaction, some of the trace corrections can even be null. This is the case, for instance, when ρ_E is an electromagnetic field's coherent state $|\alpha\rangle$ and E_n are annihilation operators, in which case the two first terms in the dissipative part of the dynamics vanish.

Finally, notice that there may have an infinite amount of environment states, as well as interactions, that provide the same evolution for the system S. It suffices to make sure that the trace corrections are such that the RHS of (3.13) is invariant under such redefinitions. In what follows, we shall explore this symmetry to explore new paradigms for the charging of quantum batteries.

3.4 Evolution under environmental measurements

(*Phys. Rev. Research 6, L042055*)

Once the basic concepts of open quantum systems have been established, we proceed to describe the scenario where the stroboscopic evolution of S is regarded. This is so, as previously discussed, whenever the environment is probed by some external detector system D which we deem controllable. By performing different sets of measurements on E, therefore, we may control the back action on the evolution of S, much in the same spirit as we did in the example provided in subsection 3.1.1. Clearly, the details about the measurements to be performed on E can only be provided after the nature of the global system is specified but, for the sake of generality, we begin our description in a broad and general framework.

Following closely the example discussed previously, we begin by assuming that the

global system $S+E$ can be sufficiently isolated from spurious detector systems of the universe set, except by a certain controlled D. This is to say that, at first, no redundant information is spread and the correlations between E and S are only destroyed after interaction with D, in which case the outcome of such a measurement tells the updated state of S. Let us name μ the pointer provided by the measurement of D, and J_μ the associated jump operator that updates the state of S. If the initial state of S is again ρ_S^0, the updated state after measurement is given by

$$\rho_S^{dt} = \frac{J_\mu \rho_S^0 J_\mu^\dagger}{\mathrm{Tr}_S\left(J_\mu^\dagger J_\mu \rho_S^0\right)}. \tag{3.14}$$

Here, we assume that such a measurement captures the change in E occurring within a time window dt of interaction with S. Naturally, this time interval is dictated by the strength of the interaction between system and environment. By repeating this measurement with D, and assuming that the experimental technology at disposal suffices to continuously probe such changes with maximum efficiency[2] (*i.e.*, that all the changes in E are indeed captured), the system S evolves through a sequence of stroboscopic jumps characterized by the set of ordered pointers $\{\mu_1, \mu_2, ...\}$. This set constitutes what we call a *trajectory* [64] for S, in which it passes through a sequence of states indexed by the outcome of each measurement. Naturally, all the physical properties of S can also be determined once we know the whole trajectory pointers between the beginning and the ending of the experiment.

As a first comment, notice that the ordering and the outcomes within the set $\{\mu_1, \mu_2, ...\}$ is intrinsically random, as they hinge on the measurements performed by D upon E. It means that, if we repeat exactly the same experiment, we shall end up with a different set $\{\tilde{\mu}_1, \tilde{\mu}_2, ...\}$, representing a different sequence of states that compose the system's trajectory at that realization. This also means that, at each realization, the physical

[2]This arises as a very strong hypothesis in the theory which, however, needs to be carefully addressed in a case-by-case basis.

observables associated to S must also change. We are then led to the question: is there any set of controllable measurements to be performed by D that may drive S through a set of trajectories where some desired physical observable is enhanced? This constitutes the central question which we now try to answer.

Before tackling that question, we must first define a way to characterize the set of trajectories defined by some fixed measurement strategy D. For this purpose, we choose the *average* trajectory as a representative of each set. This can be calculated simply by taking the average among all the possible outcomes at each step:

$$\tilde{\rho}_S^{dt} = \frac{\sum_\mu J_\mu \rho_S^0 J_\mu^\dagger}{\mathrm{Tr}_S\left(\sum_\mu J_\mu^\dagger J_\mu \rho_S^0\right)}. \tag{3.15}$$

As we have seen in our discussion of open quantum systems, in the averaged evolution for S (3.12), the jump operators J_μ are proportional, in general, to a linear combination of the interaction operators acting on S. Furthermore, they also carry the coupling strengths corrected by the environmental state. Also notice that, once the set of measurements performed by D is a POVM, the back action jump operators must satisfy the closure relation, which makes the denominator in (3.15) become unit. However, this also means that we need to include in the set of jump operators the one describing the evolution of the system when no change is detected in E. In this case, since nothing changes in E, only a free Hamiltonian evolution drives S, together with a small correction accounting for the no-change interaction.

As a consequence of (3.13), the jump operators are proportional to $\sim \sqrt{dt}$ and we can write:

$$J_\mu = \sqrt{dt} L_\mu, \ \forall \mu \neq 0, \tag{3.16}$$

$$J_0 = 1 - iHdt - dt \sum_{\mu \neq 0} \frac{L_\mu^\dagger L_\mu}{2}. \tag{3.17}$$

It is straightforward to check that this satisfies the POVM closure relation previously mentioned $J_0^\dagger J_0 + \sum_{\mu\neq 0} J_\mu^\dagger J_\mu = 1$. Whenever the pointer 0 is detected, the system is corrected by the action of the *no-jump* operator J_0, while any other pointer accounts for the respective correction in the state of S.

If we expand (3.15) using the above parametrizations, we find that

$$\tilde{\rho}_S^{dt} = \rho_S^0 - idt[H, \rho_S^0] + dt \sum_{\mu\neq 0} \left(L_\mu \rho_S^0 L_\mu^\dagger - \frac{1}{2}\{L_\mu^\dagger L_\mu, \rho_S^0\} \right). \tag{3.18}$$

Again, a Markovian master equation can be found for the average evolution $\tilde{\rho}_S$ if we repeat all the reasoning already made previously. In the weak coupling regime, the Lindblad master equation that describes the evolution for the average trajectory is given, in the Schrodinger picture, by

$$\frac{d\tilde{\rho}_S}{dt} = -i[H, \tilde{\rho}_S] + \sum_\mu L_\mu \tilde{\rho}_S L_\mu^\dagger - \frac{1}{2}\{L_\mu^\dagger L_\mu, \tilde{\rho}_S\}, \tag{3.19}$$

where in the above sum we have restricted μ to the non-zero outcome measurements.

A brief comment about the average trajectory is that indeed it may not be a real trajectory followed by the system. Instead, it serves as a good representative of the whole set of possible trajectories, around which the single-realization real trajectories orbit and, therefore, we may use it in order to answer to our main question about the existence and feasibility of environmental measurements that enhance some desired physical property.

This kind of measurement has been proposed for some specific physical platforms before, as for instance to allow for universal quantum computation [65]. Also, environmental measurements have been employed in specifically engineered reservoirs in order to maintain or even create entanglement between qubit states [66]. The protocol we develop and explore in the future sections allows for the generalization and expansion of these applications.

3.4.1 Optimization tasks

In general, optimization tasks in the engineering of quantum systems deal with practical ways to exploit some kinds of resources present in the quantum state that can be useful to achieve better values for some figures of merit. This is the case of energy and ergotropy for quantum batteries, for example.

As we have seen in the derivation of (3.19), the Lindblad operators L_μ are directly linked to the jump operators J_μ that act on the system's state as back action of the environmental measurements and, therefore, are ultimately defined by the POVM performed on E. This way, by changing the POVM we alter the family of possible trajectories followed by the system and this is reflected in a different set of L_μ's that guide the average evolution. To this point of view, the only common resources that are actually being exploited by the different sets of POVMs are those which are present in the initial state only: after the first interaction, the sole action of the measurements alters the amount of resources present in the system between two different sets. For most of applications, this is enough. However, we would like to design some protocol where, at least on average, the same amount of resource is present in the system, and we only change the ways to better extract them at each realization.

Following this guideline, we would like to find the best set of environmental POVMs for some physical task but keeping the evolution of the density matrix of S averagely unaltered. In this way, we accomplish our goal of enhancing the time evolution of some desired figure of merit, but without intrinsically altering the (average) amount of resource encoded in the system's density matrix. Mathematically, this implies in finding some transformation acting on the set of Lindblad operators that keep the evolution for $\tilde{\rho}_S(t)$ invariant. It turns out that this type of transformation is already known for some time.

3.5 Lindbladian invariant transformations

The mathematical symmetries of the GKSL master equation have been known since the first derivations made by Gorini, Kossakowski and Sudarshan [67], and independently by Lindblad [68], and they have ever since played a mathematical and computational role in the evaluation of quantum open system dynamics. They are composed of transformations acting on the set of Lindblad operators as

$$L_\mu \;\rightarrow\; L_\mu^{'} = \sum_\nu U_{\mu\nu} L_\nu + \Gamma_\mu \mathbb{1}. \tag{3.20}$$

These transformations carried in (3.19) may keep the form of the differential equation unaltered provided that the Hamiltonian of the system is also changed by

$$H \;\rightarrow\; H^{'} = H + \delta H, \tag{3.21}$$

where δH is given by

$$\delta H = \sum_{\mu,\nu} \frac{1}{2i} (\Gamma_\mu^* U_{\mu\nu} L_\nu - \Gamma_\mu U_{\mu\nu}^* L_\nu^\dagger) + \phi. \tag{3.22}$$

It is important to say that this set of transformations acting on the pair (H, L_μ) defines a group of symmetry, *i.e.*, it satisfies all the group properties for any arbitrary pairs (H, L_μ), $(H^{'}, L_\mu^{'})$. Moreover, they are also *local* in time, which means that the invariance is still valid whenever the parameters $U_{\mu\nu}$, Γ_μ and ϕ are functions of time. In what follows, we shall stick to Einstein's summation convention to avoid cumbersome and unnecessary summation signs.

The existence of such invariance property, hereafter named *Lindbladian invariance transformation* (LIT), shines some light onto our original task: since different sets L_μ are associated to different environmental POVMs, changing the pair (H, L_μ) to another LIT-invariant pair is associated to a different set of measurements performed on E. Since

this transformation is LIT, it means that the average amount of resource is also kept fixed in $\tilde{\rho}_S$ and we only optimize for the ability to better exploit them. We then work on reverse engineering: once we establish the desired form of the pair (H, L_μ), we deduct from the form of the associated jump operators (J_0, J_μ) what the carried environmental POVM should be. This reverse engineering, however, is not necessarily straightforward once it is highly dependent on the details of the implementation.

What is the physical meaning associated to the existence of such transformations? As we have seen, the emergence of different pairs (H, L_μ) arises, in our description, from the different ways in which the environment can be probed for pieces of information about S. In a general perspective, changing these probes accounts for changing how the total amount of energy and information, present in the global state, is distributed between S and E. Since, in most of the real physical applications, the presence of the environment is unavoidable, applying this optimization protocol actually thrives on what is generally taken as the cause of deleterious effects. The drawback in this case is that we need to assume perfect control and measurement over the environment's degrees of freedom.

3.5.1 Optimization protocol

As we have seen, the average trajectory is kept invariant under the action of the LIT invariance group. However, physical quantities that depend on H and/or L_μ may not be invariant as well, and a natural question arises: can one exploit this non-invariance to probe relevant phenomena or to enhance physical protocols? In other words, consider a physical quantity $\mathcal{F}(t) = \mathcal{F}[H(t), L_\mu(t), \tilde{\rho}_S(t), O(t)]$, defined as a functional of the system's operators and eventually of one or more LIT-invariant operators $O(t)$. If $\mathcal{F}(t)$ is not invariant under LIT, it means that different sets (H', L'_μ) may generate $\mathcal{F}'(t) = \mathcal{F}[H'(t), L'_\mu(t), \tilde{\rho}_S(t), O(t)] \neq \mathcal{F}(t)$ for the same set of trajectories characterized by $\tilde{\rho}_S(t)$. In this case, the value $\mathcal{F}'(t)$ will explicitly depend on the values of $(U_{\mu\nu}(t), \Gamma_\mu(t), \phi(t))$ and a specific set of such parameters can be chosen in order to opti-

mize $\mathcal{F}^{'}(t)$ for some task.

Once the physical scenario is established and the mathematical optimization problem solved, the next step is to find how to experimentally implement the optimal POVM strategy. As previously stated, the particularities of the implementation depend on the limitations and specificities of each platform. If discrete changes in the environment can be continuously monitored under the assumptions previously laid, the most general redefinition on the POVM corresponds to changing the set of jump operators as $J_\mu \rightarrow J_\mu^{'} = U_{\mu\nu}J_\nu + \sqrt{dt}\Gamma_\mu$, while the no-jump operators changes as $J_0 \rightarrow J_0^{'} = 1 - iH^{'}dt - \frac{dt}{2}L_\mu^{'\dagger}L_\mu^{'}$, with the new system's Hamiltonian $H^{'}$ as prescribed in (3.21) and (3.22).

Finally, note that finding the optimal strategy can be a very difficult problem given that it involves optimizing over infinite sets of parameters in each time step of the system's evolution. This task, however, may be simplified by imposing restrictions. For example, some sets may be impossible to implement in a specific experimental setup whereas, sometimes, the task itself may require simpler optimizations. In what follows, we discuss two examples related to the framework of quantum batteries.

3.6 Optimizations on the charging of QBs

In this final section of the chapter, we dispose two examples where the proper environmental monitoring can enhance the charging of atomic quantum batteries. In what follows, we describe the impacts of environmental monitoring on the two main figures of merit which are of interest for this quantum technology: charging power and ergotropy.

3.6.1 Charging power in small quantum systems

A clear-cut example of the application of environmental measurements in the developed protocol is the temporal charging performance achievable in a quantum battery. By definition, the power of charging in the average trajectory is given by the expression

$$\tilde{\mathcal{P}} = \frac{d}{dt}\,\mathrm{Tr}_S(H(t)\tilde{\rho}_S(t)), \tag{3.23}$$

where the explicit dependence on $H(t)$ makes it clear that this physical quantity is not LIT-invariant. Naturally, this quantity represents an average over all the power values obtained when the experiment is repeated and the system is driven through a fixed set of trajectories which average is given by $\tilde{\rho}_S(t)$. Henceforth, this realization shall not be stressed again.

In particular, one can ask which measurement strategy maximizes or minimizes the power in the system by calculating $\tilde{\mathcal{P}}(t)$ for all possible alternatives. In this case, a change on the set $(H, L_\mu) \to (H', L'_\mu)$ causes a change in the power given by

$$\tilde{\mathcal{P}}'(t) = \partial_t\,\mathrm{Tr}_S(H'(t)\tilde{\rho}_S(t)) = \tilde{\mathcal{P}}(t) + \partial_t\,\mathrm{Tr}_S(\delta H'(t)\tilde{\rho}_S(t)), \tag{3.24}$$

where $\delta\tilde{\mathcal{P}}(t) \equiv \partial_t\,\mathrm{Tr}_S(\delta H'(t)\tilde{\rho}_S(t))$ is the power extra contribution due to the redefinition of the measurement strategy. Notice that, according to (3.22), this term depends solely on the parameters that define the new set of trajectories followed by the system. Some straightforward calculations [69] using (3.19) lead to the final form for $\delta\tilde{\mathcal{P}}(t)$:

$$\delta\tilde{\mathcal{P}}(t) = i\,\langle[H, \delta H]\rangle + \Re\,\langle L_\mu^\dagger[\delta H, L_\mu]\rangle + \langle\partial_t \delta H\rangle\,. \tag{3.25}$$

Here, $\Re$ stands for the real part of the average value $\langle A\rangle \equiv \mathrm{Tr}_S(A\tilde{\rho}_S)$. Notice that, written in this format, the extra power can be calculated as a function of the LIT parameters once the original pair (H, L_μ) is fixed. This pair is the one responsible for selecting the desired average evolution of the system. It can be picked, for instance, from any previously known evolution which possesses some desired property encoded in the average state.

One simple example is given by a two dimensional (qubit) quantum battery coupled to a thermal bath at inverse temperature β, in which case the typical description of the

evolution is given by the set $\left(H = \frac{\omega}{2}\hat{\sigma}_z,\ L_\pm = \sqrt{\gamma_\pm}\hat{\sigma}_\pm\right)$, where $\hat{\sigma}_+$ ($\hat{\sigma}_-$) corresponds to the system losing (gaining) a quantum of energy ω to (from) the environment at rate γ_- (γ_+) and $\frac{\gamma_+}{\gamma_-} = e^{-\beta\hbar\omega}$. This system has a very well-known behaviour with an asymptotic state given by a Gibbs distribution with Hamiltonian H and temperature β. For this mean evolution, the most general transformation on the Lindblad operators results in

$$\delta H = \Re(\alpha)\hat{\sigma}_x - \Im(\alpha)\hat{\sigma}_y, \tag{3.26}$$

where $\alpha = -i(\Gamma_\mu^* U_{\mu+}\sqrt{\gamma_+} - \Gamma_\mu U_{\mu-}^*\sqrt{\gamma_-})$ is a complex number defined by the chosen measurement strategy. Here, the eventual time dependence of the parameters is implied. Also, note that δH is defined on the plane perpendicular to H in the Bloch sphere.

For simplicity, let us now restrict ourselves to the set of parameters where $\alpha(t) = |\alpha|e^{i\theta(t)}$, with $|\alpha|$ constant. After some algebra, one obtains an extra contribution for the power of system S given by

$$\delta\tilde{\mathcal{P}} = \frac{\alpha(t)}{2}\left[i(\omega + \dot{\theta}) - \frac{\gamma_+ + \gamma_-}{2}\right]\tilde{\rho}_{ge}(t) + h.c., \tag{3.27}$$

where $\tilde{\rho}_{ij}(t) = \langle i|\,\tilde{\rho}_S(t)\,|j\rangle$ stands for the coherence of the system ($i \neq j$) in the eigenbasis of H. Note that, in this example, the final form of (3.27) indicates a physical interpretation to each strategy: when the time variation of the internal energy of the qubit is considered, a general transformation on the set (H, L_μ) acts as a transferrer, which transforms the evolution of the initial coherences in the system into an energy flow contribution at each time t.

In particular, if the system has no initial coherence in the eigenbasis of H, then $\rho_{eg}(t) = 0$ throughout the evolution and the choice of measurement strategy is irrelevant. Also note that the choice of the best LIT, encoded in $\alpha(t)$, depends on the phase of $\rho_{ge}(0)$. In fact, one can choose the sign of $\delta\tilde{\mathcal{P}}(t)$ by simply changing the relative phase between $\alpha(t)$ and $\rho_{ge}(0)$. Finally, Eq. (3.27) indicates that one can find monitoring schemes

where the exchanged energy per unit of time between system and its environment can be controlled for any desired task at the expense of any coherence present in the system's initial state.

Figure 3.1 shows the power and internal energy of the qubit for different parameters. The black curve corresponds to $\alpha = 0$, i.e. the original set (H, L_μ). The coloured curves correspond to different sets, where $|\alpha|$ is kept fixed and θ changes linearly in time. The lightblue curve corresponds to a time independent strategy, where the time evolution of the coherences naturally creates the oscillatory behaviour in the system's internal energy. In this case, θ only defines the initial phase of the oscillation. On the other hand, by allowing θ to change in time one is able to coherently interfere either constructively (red, dashed curve) or destructively (orange, dot-dashed curve) with the time oscillations of the coherences of the qubit, accelerating or decelerating the rate at which energy is pumped into the system through the environment.

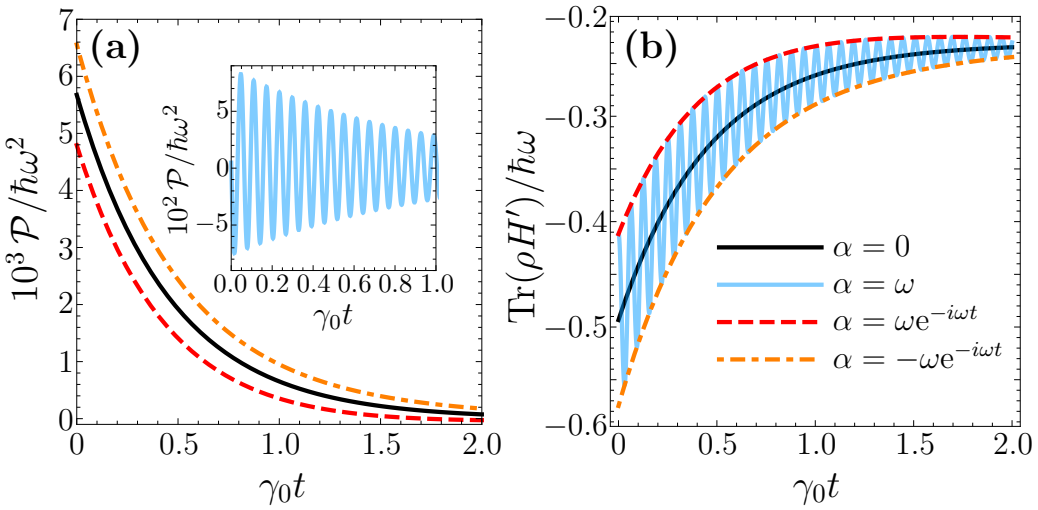

Figure 3.1: Time evolution of (a) power and (b) internal energy for different measurement strategies leading to the same evolution of a qubit. In all curves, $\gamma_0 = 10^{-2}\omega$, $k_B T_0 = 0.2\hbar\omega$ and $k_B T_f = \hbar\omega$.

In all curves, an initial pure state $|\psi_0\rangle = \sqrt{p_g^0}\,|g\rangle + \sqrt{p_e^0}\,|e\rangle$ evolves through the same $\tilde{\rho}_S(t)$ and asymptotically reaches a Gibbs state $\tilde{\rho}_S^{as} = p_g^f |g\rangle\langle g| + p_e^f |e\rangle\langle e|$ where p_i^j is given by a Boltzmann distribution with energy $E_i = \langle i|\, H\, |i\rangle$ and inverse temperature β_j. We

are also considering jump ratios $\gamma_+ = \gamma_0 \overline{n}$ and $\gamma_- = \gamma_0(\overline{n}+1)$, where $\overline{n} = (1 - e^{-\beta_f \hbar\omega})^{-1}$.

Notice that, in the time independent strategy (lightblue curve), the time oscillations of the energetic coherences in the system naturally average to the original set of measurements given by (H, L_μ), which reflect that, in order to achieve better figures of merit in a consistent way, time adaptability on the measurements scheme needs to be taken into account. Finally, also notice that all curves converge in asymptotic times, as a consequence of the vanishing energetic coherences in the final Gibbs state.

3.6.2 Ergotropy on a quantum battery

Another example of non LIT invariant quantity is the ergotropy stored in a quantum battery. Recalling its definition previously presented, the maximum amount of energy that can be extracted from the system via unitary transformations is given by

$$\mathcal{E}[H, \tilde{\rho}] = \sum_i \tilde{p}_i^{dec} \left(\langle \tilde{p}_i^{dec} | \, H \, | \tilde{p}_i^{dec} \rangle - E_i \right), \tag{3.28}$$

where the *dec* superscript tells that the eigenvalues of the density matrix $\tilde{\rho}$ must be ordered in decreasing order, while the eigenvalues E_i of H are ordered increasingly. The form of this equation again makes it explicit that the ergotropy is also a non-invariant physical quantity, as a function of H, and therefore it may change as a consequence of a Lindbladian invariance transformation.

For instance, consider again the same qubit subjected to a thermal bath of inverse temperature β, for which the asymptotic state is the same Gibbs state previously described, $\tilde{\rho}_{ii}^{as} = \frac{e^{-\beta E_i}}{\sum_{j=g,e} e^{-\beta E_j}}$. Given that $\tilde{\rho}_{ee}^{as} < \tilde{\rho}_{gg}^{as}$, $\tilde{\rho}^{as}$ has no stored ergotropy with relation to the Hamiltonian H, which can be straightforwardly checked from its definition given above. This is not necessarily true, however, if a different pair $(H^{'}, L_\mu^{'})$ is picked to drive the dynamics. The change in the Hamiltonian of the system means that $\tilde{\rho}^{as}$ and $H^{'} = H + \delta H$ will not commute anymore and, as a consequence, $\tilde{\rho}^{as}$ may store ergotropy with respect to the new Hamiltonian.

The eigenstates of $H^{'}$ are written in terms of the original eigenstates as

$$|\psi_{+}\rangle = \sqrt{n_1}\,|g\rangle + e^{-i\theta}\sqrt{n_2}\,|e\rangle\,, \tag{3.29}$$

$$|\psi_{-}\rangle = \sqrt{n_2}\,|g\rangle - e^{-i\theta}\sqrt{n_1}\,|e\rangle\,, \tag{3.30}$$

with the eigenvalues $E_{\pm} = \pm\frac{\omega}{2}\,(2G(\alpha)+1)$, where

$$G(\alpha) \equiv \frac{1}{2}\sqrt{1+\frac{|\alpha|^2}{\omega^2}} - \frac{1}{2}, \tag{3.31}$$

$n_1 = \frac{G(\alpha)}{2G(\alpha)+1}$ and $n_2 = \frac{G(\alpha)+1}{2G(\alpha)+1}$. It is very easily checked that for $\alpha \to 0$ (*i.e.*, no change in the strategy) we recover the original states.

After LIT, the transformed ergotropy is given by

$$\mathcal{E}[H^{'}, \tilde{\rho}^{as}] = G(\alpha)\hbar\omega\left(\tilde{\rho}^{as}_{gg} - \tilde{\rho}^{as}_{ee}\right). \tag{3.32}$$

Note that the addition of δH per se does not change the asymptotic value of the internal energy of the system, since the new Hamiltonian δH is completely off-diagonal in the eigenbasis of $\tilde{\rho}^{as}$, implying that $\mathrm{Tr}_S(\tilde{\rho}^{as}H^{'}) = \mathrm{Tr}_S(\tilde{\rho}^{as}H^{'})$. This indicates that no extra energetic resource is being transmitted into the system by δH. However, $\tilde{\rho}^{as}$ is not a thermal equilibrium state anymore and the energy to keep it out of equilibrium and, therefore, to store ergotropy in it, is injected by the transformed environment.

3.6.3 Implementation on photonic environments

As mentioned before, each set (H, L_μ) can be associated to a particular physical implementation of quantum trajectories, each one corresponding to a set of jump operators acting on the system and depending on measurements performed over the environment. In particular, let us discuss a simple implementation of the different POVMs on the environment degrees of freedom in the case where a two-level system is in contact with a

thermal-like environment. The respective engineering works as in Fig. 3.2: a three-level atom with levels $|g\rangle$, $|e\rangle$ and $|m\rangle$ and spontaneous decay rates γ_- in the $|e\rangle \to |g\rangle$ transition and Γ in the $|m\rangle \to |e\rangle$ transition may be coherently pumped with a strong field Ω in the $|g\rangle \leftrightarrow |m\rangle$ transition. If $\Omega \ll \Gamma$, two time-scales are established in the system: the coherent pumping of $|g\rangle$'s population to level $|m\rangle$ is a slow process, while the decay $|m\rangle \to |e\rangle$ is a fast one. The net effect is that level $|m\rangle$ is adiabatically eliminated from the dynamics, and an effective incoherent pump from level $|g\rangle$ to level $|e\rangle$ takes place with rate $\gamma_+ = 4\Omega^2/\Gamma$.

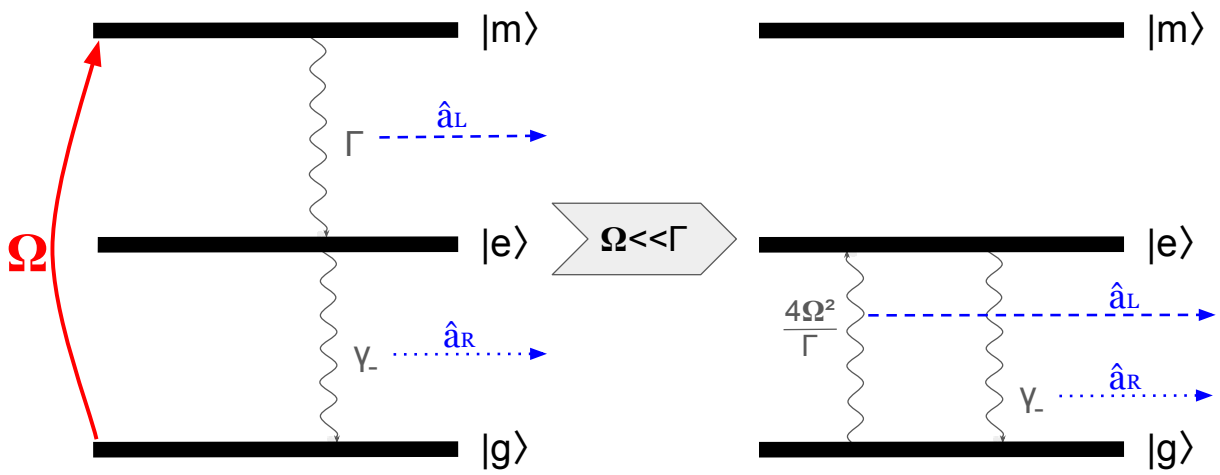

Figure 3.2: Example of reservoir engineering which allows the association of a leaked photon, circularly polarized to the left (right), to the $|g\rangle \to |e\rangle$ ($|e\rangle \to |g\rangle$) jump of the system. In this engineering, level $|m\rangle$ is adiabatically eliminated from the dynamics and the qubit is encoded in the two lowest lying levels.

The emission of two different photons serves as a marker to the which-path information related to the respective jumps happening within the time window dt of interaction. Detection of the left (right) polarization implements $\hat{\sigma}_+$ ($\hat{\sigma}_-$) on the system. However, by mixing the which-path information encoded in this modes' polarization prior to its

detection allows us to implement different jump operators in the system. In what follows, Fig. 3.3 shows the implementations of two different sets of jump operators on the qubit: by making use of a quarter wave plate followed by a 50/50 polarized beam splitter prior to a photon-counting detector allows us to completely follow the which-path information encoded in the optical path of the leaked photon. However, if we remove the QWP and shine the photon directly into the PBS, the which-path information is maximally mixed in the output optical paths of each detector. This implements the $U_{\mu\nu}$ part of the new POVM strategy.

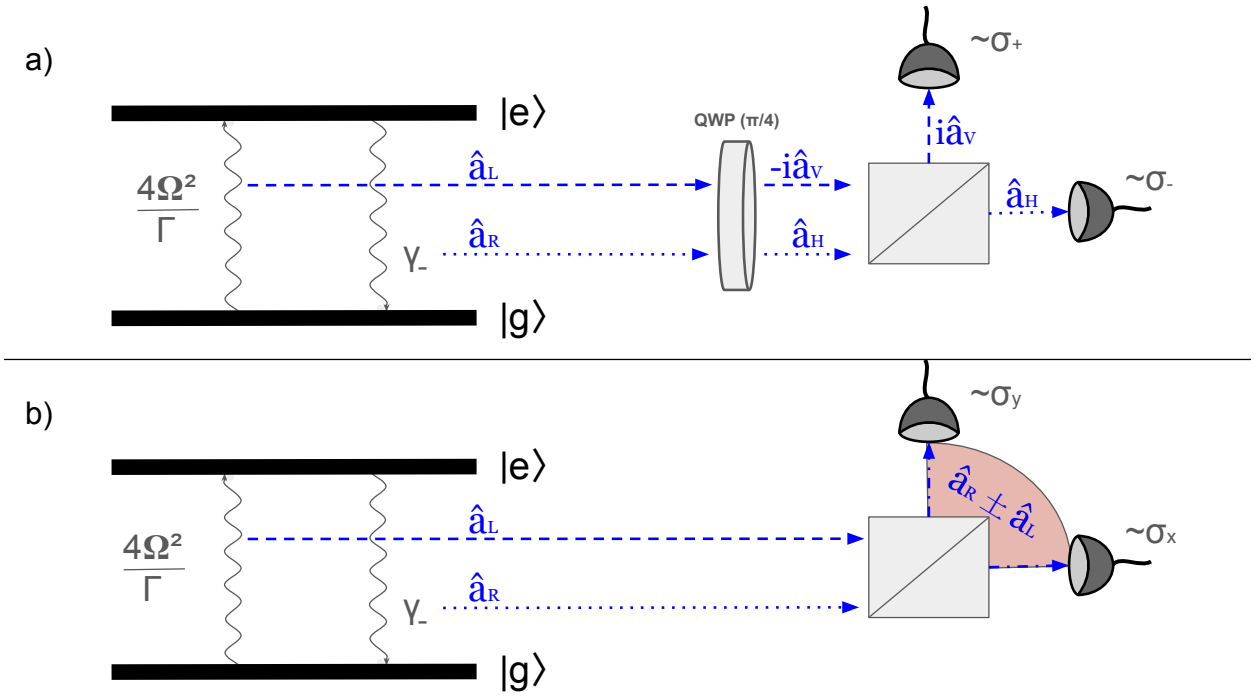

Figure 3.3: Description of two possible environmental POVMs: associating the leaked photon's polarization to different jumps happening in the system allows us to probe the former in different ways, which therefore change the effective trajectory of the latter. In (a) the which-path information directly associates the detected optical path to $\hat{\sigma}_{\pm}$ jumps, while in (b) we maximally mix the encoded information about the jump prior to its detection, therefore guiding the system through a different set of trajectories defined by the Lindblad operators $\hat{\sigma}_{x/y}$.

On the other hand, combining each mode with a local oscillator field (a coherent state of amplitude s_μ) at a highly reflective mirror (of reflectivity $r \approx 1$), implements the addition of the Γ_μ term in the same transformation, where $\Gamma_\mu \propto \sqrt{1-r} \times s_\mu$. This is

illustrated in Fig. 3.4.

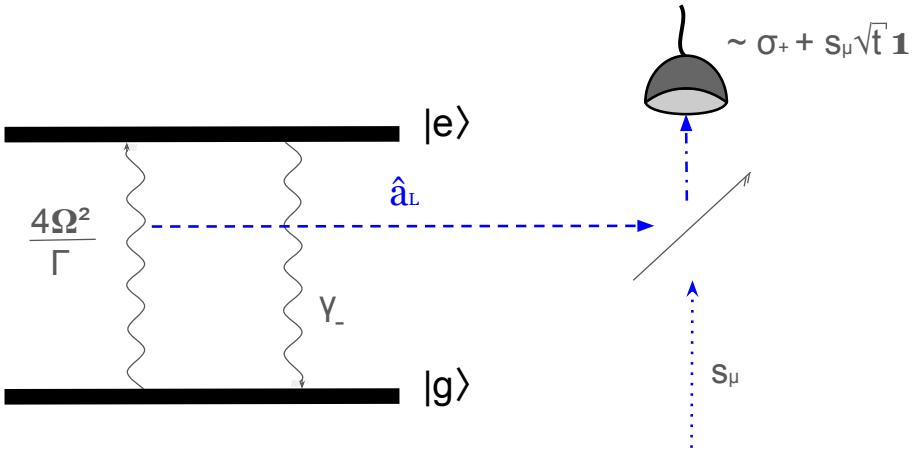

Figure 3.4: Combining a leaked mode of the environment with an external photon source at a highly reflective mirror allows us to implement the non-homogeneous part of the transformation.

The logic behind this implementation is simple: the rotation of the polarization recombines the modes and therefore the jumps to which they are associated, whereas their combination with the local oscillator at the highly reflective mirror superposes the modes with an external photon source in such a way that a click on a given detector imposes a superposition of a corresponding jump (the photon coming from the system) and identity (the photon coming from the external source) acting on the system. Finally, an external classical field directly driving the $|g\rangle \leftrightarrow |e\rangle$ transition implements the required δH to complete the set for the new strategy.

3.7 Overview

In this section, we have proposed a systematic protocol to explore symmetries in quantum Markovian master equations beyond their mathematical elegance. It consists of identifying

physical quantities that are not invariant under symmetry transformations of the GKSL master equation and searching for the particular form of that equation that optimizes a given practical physical task. The asymptotic stored energy and the energy flux through the evolution of a low-dimensional quantum system were the two examples depicted here but the protocol is general and any figure of merit that varies according to a chosen form is suitable for optimization. Further examples to be explored in the future include heat exchanged with the environment, entropy production, efficiency of thermal machines, preparation of target oriented asymptotic states, etc.

This method is a fresh approach into the mathematical symmetries of the Lindblad master equation: in contrast to previous schemes, here the average evolution of $\tilde{\rho}_S(t)$ and, therefore, the information encoded in it through time, is unchanged by design. Rather, we optimize for the ability to better extract a certain physical quantity from a fixed time evolution. From a fundamental point of view, this shows that the same sequence of quantum states can correspond to different trajectories in some parameter space that involves quantities that are not invariant to symmetry transformations. It also means, from a practical point of view, that these transformations can be used to optimize tasks that depend on such quantities.

This is particularly useful whenever the presence of the environment is unavoidable and one needs to save resources throughout a given fixed dynamics, or when dissipative dynamics are essential to perform a given task. The latter is true, for instance, in protocols that rely on intermediate steps such as optical pumping, electromagnetic induced transparency and coherent population trapping, to name a few. This method is particularly well adapted to these cases. This is certainly a novel approach to an equation that has been extensively studied over the spam of five decades and one that has potential practical aspects.

The method also allows to identify the resource whose consumption is being optimized. In the examples worked on the paper, power requires initial quantum coherence to be

consumed throughout the evolution whereas the storing of ergotropy comes from the athermality of the asymptotic state. The identified resources are consistent with previous results found in the literature [70–75].

In addition, the unravelling of the GKSL equation in terms of quantum trajectories already points to the experimental way to probe the optimization method. In fact, finding the optimal strategy parameters automatically provides the best set of environmental measurements that must be carried on. This meets direct applications in any area where engineering and control of a given reservoir can be explored to enhance physical protocols, as well as areas where continuous monitoring of the environment is performed in order to feedback control a given evolution. Note that, nowadays, there are plenty of atomic (real and artificial) systems where the conditions for such experiments are met, including atoms coupled to open cavities [76–78], superconducting qubits connected to waveguides [79], quantum dots embedded in nanowires [80], NV-centers in photonic crystals [81], etc.

Finally, a first idea on how to generalize this protocol starts by wondering about the effects of letting the LIT parameters assume arbitrary time dependences, which is allowed by the symmetries involved. Furthermore, I also let open the question whether this procedure could be performed on other types of master equations, such as those describing non-Markovian evolutions or even master equations describing classical systems. At last, it may also be of interest to study the relations between these symmetries and their applications with fundamental physical questions related to the thermodynamics of quantum systems.

Follow-ups

Throughout this thesis we have delved into the area of quantum batteries. As the name suggests, this amounts for applications of microscopic systems that can store, and later deliver, some defined amount of energy *on demand*. This area of research has attracted the interests of many due to its appeal as the necessity to address new energetic resources rises in a modern, interdisciplinary paradigm [82]. This final chapter will be dedicated to present the natural follow-ups of the three main papers presented in the scope of this thesis.

As we have investigated the advantages of exploring the quantum vacuum of a single-moded electromagnetic field, the natural question which arises is: what if we replace the classical power source mode by another quantized version of this field? In this case, under the same adiabatic elimination conditions already explored, this tripartite system presents a hybrid mix of Jaynes-Cummings and anti-Jaynes-Cummings effective Hamiltonian which can be exactly diagonalized and where excitations are spread and shared by the three quantum systems. In this scenario, multiple things can be investigated: what is the asymptotic state for each individual system? And for any bipartite system? Is there any particular initial state for the atom that entangles the two modes? Conversely, is there any choice of parameters for the modes' initial states that can help in purifying the atomic state? What is the most that can be done to the atom's state if we regard it as quantum battery? Interestingly enough, this kind of system has a feasible experimental realization using crossed cavities [83–85].

In the open quantum system scenario, on the other hand, one possible research path

for the application of the developed mathematical techniques is on the investigation of finite time measurements. Namely, if some experimentalist is tracking the evolution of system S by probing its environment, the most crucial approximation in order to tell that the outcome data indeed reproduces the actual system's state is the infinitesimal time window of the environmental measurement. If the carried measurement actually takes some time window $d\tau$ which is bigger than the typical system/environment interaction time window dt, then one is only able to follow some rough, stroboscopic images of the system S. In this paradigm, assuming that the measurement process is non-timely optimal, what is the best that can be done in order to retrieve (the most of) the system's actual properties? Or, conversely, is there any way to find the real dynamics involved in the system+environment interaction given that we are only allowed to a rough estimative map of the real evolution of S? Indeed, we may even consider other types of imperfect coarse-graining which are not only timely. If the employed detector system D has some minimal energetic window, which renders it the inability to differentiate two types of jumps happening in the environment (for instance, it is unable to differ a photon of energy $\hbar\omega$ from another with energy $\hbar(\omega + \delta)$ for some small, fixed δ), can we retrieve some fiducial imaging of what is actually happening to the system over time? What is the best kind of measurement that, in this case, circumvents most of the detector's inability?

Finally, also notice that the above raised questions can be directly connected to different questions of metrological interest. For instance, given that some parameter is encoded in the open evolution, probing the systems' dynamics may furnish an estimative to it. However, if our measurement is imperfectly coarse-grained, how can we account for a better estimation in this scenario? These are some of the questions which arose as natural, interesting follow-ups from this set of investigations and, therefore, should be addressed in future works.

Bibliography

[1] Ferreira, V.S., Kim, G., Butler, A. et al. *Deterministic generation of multidimensional photonic cluster states with a single quantum emitter*. Nat. Phys. 20, 865?870 (2024). DOI: 10.1038/s41567-024-02408-0; 1

[2] Merlin Cooper, Laura J. Wright, Christoph Soller, and Brian J. Smith. *Experimental generation of multi-photon Fock states*. Opt. Express 21, 5309-5317 (2013); 1

[3] Cao, H. and Hansen, L. M. and Giorgino, F. and Carosini, L. and Zahálka, P. and Zilk, F. and Loredo, J. C. and Walther, P. *Photonic Source of Heralded Greenberger-Horne-Zeilinger States*. Phys. Rev. Lett. 132 **13** (2024). DOI: 10.1103/PhysRevLett.132.130604. 1

[4] C. J. Hood, T. W. Lynn, H. Mabuchi, M. S. Chapman, J. Ye, and H. J. Kimble. *Real-time cavity QED with single atoms*. International Quantum Electronics Conference, P. Corkum and N. Peyghambarian, eds., Vol. 7 of OSA Technical Digest (Optica Publishing Group, 1998), paper QMC1; 1

[5] H. Walther. *Laser manipulation and cavity QED with trapped ions*. AIP Conf. Proc. 11 June 1999; 477 (1): 179?196. DOI: 10.1063/1.59356; 1

[6] Dowling Jonathan P. and Milburn Gerard J. (2003). *Quantum technology: the second quantum revolution*. Phil. Trans. R. Soc. A.361: 1655?1674. DOI: 10.1098/rsta.2003.1227; 1

[7] Aspect, A. (2023). *The Second Quantum Revolution: From Basic Concepts to Quantum Technologies*. In Photonic Quantum Technologies, M. Benyoucef (Ed.). DOI: 10.1002/9783527837427.ch2; 1

[8] Boixo, S., Isakov, S. V., Smelyanskiy, V. N., Babbush, R., Ding, N., Jiang, Z., and Neven, H. (2018). *Characterizing Quantum Supremacy In Near-term Devices*. Nature Physics, 14(10), 1050-1057; 1

[9] Nielsen, M.A. And Chuang, I.L., 2010. *Quantum Computation And Quantum Information*. Cambridge University Press; 1

[10] Xi, Z., Li, Y. and Fan, H. Quantum coherence and correlations in quantum system. Sci Rep 5, 10922 (2015). DOI: 10.1038/srep10922. 1

[11] Kuroiwa, Kohdai and Takagi, Ryuji and Adesso, Gerardo and Yamasaki, Hayata. *Every Quantum Helps: Operational Advantage of Quantum Resources beyond Convexity*. Phys. Rev. Lett. 132, 150201 (2024); 1, 80

[12] Wootters William K. (1998). *Quantum entanglement as a quantifiable resource*. Phil. Trans. R. Soc. A.356: 1717?1731. DOI: 10.1098/rsta.1998.0244; 1, 80

[13] Chitambar, Eric and Gour, Gilad. *Quantum resource theories*. Rev. Mod. Phys. 91, 025001 (2019); 1, 80

[14] Tetienne, JP. *Quantum sensors go flat*. Nat. Phys. 17, 1074?1075 (2021); 2

[15] Thomas-Peter, Nicholas and Smith, Brian J. and Datta, Animesh and Zhang, Lijian and Dorner, Uwe and Walmsley, Ian A. *Real-World Quantum Sensors: Evaluating Resources for Precision Measurement*. Phys. Rev. Lett. 107, 113603 (2011); 2

[16] Proctor, Timothy J. and Knott, Paul A. and Dunningham, Jacob A. *Multiparameter Estimation in Networked Quantum Sensors*. Phys. Rev. Lett. 120, 080501 (2018); 2

[17] Aslam, N., Zhou, H., Urbach, E.K. et al. *Quantum sensors for biomedical applications*. Nat Rev Phys 5, 157?169 (2023). DOI: 10.1038/s42254-023-00558-3; 2

[18] Fu-Guo Deng, Xi-Han Li, Chun-Yan Li, Ping Zhou, Hong-Yu Zhou. *Quantum secure direct communication network with Einstein?Podolsky?Rosen pairs*. Physics Letters A, Vol. 359, Issue 5 (2006). DOI: 10.1016/j.physleta.2006.06.054; 2

[19] Munro, W., Stephens, A., Devitt, S. et al. *Quantum communication without the necessity of quantum memories*. Nature Photon 6, 777?781 (2012). DOI: 10.1038/nphoton.2012.243; 2

[20] Wengerowsky, S., Joshi, S.K., Steinlechner, F. et al. *An entanglement-based wavelength-multiplexed quantum communication network*. Nature 564, 225?228 (2018); 2

[21] Pirandola, S. *End-to-end capacities of a quantum communication network*. Commun Phys 2, 51 (2019). DOI: 10.1038/s42005-019-0147-3; 2

[22] Bhattacharjee, S., Dutta, A. *Quantum thermal machines and batteries*. Eur. Phys. J. B 94, 239 (2021). DOI: 10.1140/epjb/s10051-021-00235-3; 2

[23] S., Vahid, S., Varinder, B., Giuliano, and R., Dario. *Micromasers as quantum batteries*. Quantum Sci. Technol. 7 04LT01 (2022). DOI: 10.1088/2058-9565/ac8829; 2

[24] C. B., Felix, V., Sai, M., Kavan and G., John. *Quantacell: powerful charging of quantum batteries*. New J. Phys. 17 075015 (2015). DOI: 10.1088/1367-2630/17/7/075015; 2

[25] Campaioli, Francesco and Pollock, Felix A. and Binder, Felix C. and Celeri, Lucas and Goold, John and Vinjanampathy, Sai and Modi, Kavan. *Enhancing the Charging Power of Quantum Batteries*. Phys. Rev. Lett. 118, 150601 (2017). DOI: 10.1103/PhysRevLett.118.150601; 2

[26] Santos, Alan C. and Çakmak, Barış and Campbell, Steve and Zinner, Nikolaj T. *Stable adiabatic quantum batteries*. Phys. Rev. E 100, 032107 (2019). DOI: 10.1103/PhysRevE.100.032107; 2

[27] Rojo-Francàs, Abel and Isaule, Felipe and Santos, Alan C. and Juliá-Díaz, Bruno and Zinner, Nikolaj Thomas. *Stable collective charging of ultracold-atom quantum batteries*. Phys. Rev. A 110, 032205 (2024). DOI: 10.1103/PhysRevA.110.032205; 2

[28] Tibben, Daniel J., Gaspera, Enrico Della, Embden, Joel van, Reineck, Philipp, Quach, James Q., Campaioli, Francesco, and Gomez, Daniel E. *Extending the self-discharge time of Dicke quantum batteries using molecular triplets*. PRX Energy (2025). DOI: 10.1103/bhyh-53np; 2

[29] Rossini, Davide and Andolina, Gian Marcello and Polini, Marco. *Many-body localized quantum batteries*. Phys. Rev. B 100, 115142 (2019). DOI: 10.1103/PhysRevB.100.115142; 2

[30] Gyhm, Ju-Yeon and Rosa, Dario and Šafránek, Dominik. *Minimal time required to charge a quantum system*. Phys. Rev. A 109, 022607 (2024). DOI: 10.1103/PhysRevA.109.022607; 2

[31] Yangyang Ge, Xiangmin Yu, Wei Xin, Zhimin Wang, Yu Zhang, Wen Zheng, Shaoxiong Li, Dong Lan, Yang Yu. *Efficient charging and discharging of a superconducting quantum battery through frequency-modulated driving*. Appl. Phys. Lett. (2023). DOI: 10.1063/5.0161354; 2

[32] Julià-Farré, Sergi and Salamon, Tymoteusz and Riera, Arnau and Bera, Manabendra N. and Lewenstein, Maciej. *Bounds on the capacity and power of quantum batteries*. Phys. Rev. Research 2, 023113 (2020). DOI: 10.1103/PhysRevResearch.2.023113; 2

[33] Alan C. Santos, Andreia Saguia, Marcelo S. Sarandy. *Stable and charge-switchable quantum batteries*. arXiv preprint (2020). DOI: arXiv:1912.03675v2; 2

[34] Salvia, Raffaele and Perarnau-Llobet, Martí and Haack, Géraldine and Brunner, Nicolas and Nimmrichter, Stefan. *Quantum advantage in charging cavity and spin batteries by repeated interactions*. Phys. Rev. Research 5, 013155 (2023). DOI: 10.1103/PhysRevResearch.5.013155; 3

[35] M. Hadipour, S. Haseli, D. Wang, S. Haddadi. *Proposed Scheme for a Cavity-Based Quantum Battery*. Adv Quantum Technol. 2024, 7, 2400115. DOI: 10.1002/qute.202400115; 3

[36] Wang, Lu and Liu, Shu-Qian and Wu, Feng-lin and Fan, Hao and Liu, Si-Yuan. *Cavity-optomechanical quantum battery*. Phys. Rev. A 110, 062204 (2024). DOI: 10.1103/PhysRevA.110.062204; 3

[37] Fainstein, A., Jusserand, B. *Raman Scattering in Resonant Cavities*. In: Cardona, M., Merlin, R. (eds) Light Scattering in Solid IX. Topics in Applied Physics, vol 108. Springer, Berlin, Heidelberg. (2006) DOI: $10.1007/978-3-540-34436-0_2$; 5

[38] L. C. Maier, J. C. Slater. *Field Strength Measurements in Resonant Cavities*. J. Appl. Phys. 1 January 1952; 23 (1): 68?77. DOI: 10.1063/1.1701980; 5

[39] E. F. Schubert, Y.?H. Wang, A. Y. Cho, L.?W. Tu, G. J. Zydzik. *Resonant cavity light?emitting diode*. Appl. Phys. Lett. 24 February 1992; 60 (8): 921?923. DOI: 10.1063/1.106489; 5

[40] M. Selim Unlu, Samuel Strite. *Resonant cavity enhanced photonic devices*. J. Appl. Phys. 15 July 1995; 78 (2): 607-639. DOI: 10.1063/1.360322; 5

[41] Francica, G., Goold, J., Plastina, F. et al. *Daemonic ergotropy: enhanced work extraction from quantum correlations*. npj Quantum Inf 3, 12 (2017). DOI: 10.1038/s41534-017-0012-8; 5

[42] Yang, Xue and Yang, Yan-Han and Alimuddin, Mir and Salvia, Raffaele and Fei, Shao-Ming and Zhao, Li-Ming and Nimmrichter, Stefan and Luo, Ming-Xing. *Battery Capacity of Energy-Storing Quantum Systems*. Phys. Rev. Lett. 131, 030402 (2023). DOI: 10.1103/PhysRevLett.131.030402; 5

[43] Campaioli, Francesco and Gherardini, Stefano and Quach, James Q. and Polini, Marco and Andolina, Gian Marcello. *Colloquium: Quantum batteries*. Rev. Mod. Phys. 96, 031001 (2024). DOI: 10.1103/RevModPhys.96.031001; 6

[44] Gemme, Giulia and Grossi, Michele and Vallecorsa, Sofia and Sassetti, Maura and Ferraro, Dario. *Qutrit quantum battery: Comparing different charging protocols*. Phys. Rev. Research 6, 023091 (2024). DOI: 10.1103/PhysRevResearch.6.023091; 6

[45] Barra, Felipe. *Dissipative Charging of a Quantum Battery*. Phys. Rev. Lett. 122, 210601 (2019). DOI: 10.1103/PhysRevLett.122.210601; 7

[46] M Carrega et al. *Dissipative dynamics of an open quantum battery*. New J. Phys. 22 083085 (2020). DOI: 10.1088/1367-2630/abaa01; 7

[47] A. E. Allahverdyan et al. *Maximal work extraction from finite quantum systems*. EPL 67 565 (2004). DOI: 10.1209/epl/i2004-10101-2; 7

[48] Francica, G. and Binder, F. C. and Guarnieri, G. and Mitchison, M. T. and Goold, J. and Plastina, F. *Quantum Coherence and Ergotropy*. Phys. Rev. Lett. 125, 180603 (2020). DOI: 10.1103/PhysRevLett.125.180603; 10

[49] Çakmak, Barış. *Ergotropy from coherences in an open quantum system*. Phys. Rev. E 102, 042111 (2020). DOI: 10.1103/PhysRevE.102.042111; 10

[50] Niu, Zhibo and Wu, Yang and Wang, Yunhan and Rong, Xing and Du, Jiangfeng. *Experimental Investigation of Coherent Ergotropy in a Single Spin System*. Phys. Rev. Lett. 133, 180401 (2024). DOI: 10.1103/PhysRevLett.133.180401; 10

[51] Hadipour, M., Haseli, S. *Work extraction from quantum coherence in non-equilibrium environment*. Sci Rep 14, 24876 (2024). DOI: 10.1038/s41598-024-75478-y; 10

[52] *D F James and J Jerke. 2007. Effective Hamiltonian theory and its applications in quantum information. Canadian Journal of Physics. 85(6): 625-632.* 15

[53] Moya-Cessa, H. and Bužek, V. and Kim, M. S. and Knight, P. L. *Intrinsic decoherence in the atom-field interaction*. Phys. Rev. A 48, 3900 (1993). DOI: 10.1103/PhysRevA.48.3900; 20

[54] Kamin, F. H. and Tabesh, F. T. and Salimi, S. and Santos, Alan C. *Entanglement, coherence, and charging process of quantum batteries*. Phys. Rev. E 102, 052109 (2020). DOI: 10.1103/PhysRevE.102.052109; 42

[55] Shi, Hai-Long and Ding, Shu and Wan, Qing-Kun and Wang, Xiao-Hui and Yang, Wen-Li. *Entanglement, Coherence, and Extractable Work in Quantum Batteries*. Phys. Rev. Lett. 129, 130602 (2022). DOI: 10.1103/PhysRevLett.129.130602; 42

[56] Arjmandi, Mohammad B. and Shokri, Abbas and Faizi, Esfandyar and Mohammadi, Hamidreza. *Performance of quantum batteries with correlated and uncorrelated chargers*. Phys. Rev. A 106, 062609 (2022). DOI: 10.1103/PhysRevA.106.062609; 42

[57] Liu, Shu-Qian and Wang, Lu and Fan, Hao and Wu, Feng-Lin and Liu, Si-Yuan. *Better performance of quantum batteries in different environments compared to closed batteries*. Phys. Rev. A 109, 042411 (2024). DOI: 10.1103/PhysRevA.109.042411; 48

[58] Xu, Kai and Zhu, Han-Jie and Zhang, Guo-Feng and Liu, Wu-Ming. *Enhancing the performance of an open quantum battery via environment engineering*. Phys. Rev. E 104, 064143 (2021). DOI: 10.1103/PhysRevE.104.064143; 48

[59] Breuer, Heinz-Peter, and Francesco Petruccione. *The Theory of Open Quantum Systems* (Oxford, 2007; online edn, Oxford Academic, 1 Feb. 2010). DOI: 10.1093/acprof:oso/9780199213900.001.0001; 49

[60] Richard J Cook. *What are Quantum Jumps?* Phys. Scr. 49 (1988). DOI: 10.1088/0031-8949/1988/T21/009; 55

[61] Sauter, Th. and Neuhauser, W. and Blatt, R. and Toschek, P. E. *Observation of Quantum Jumps*. Phys. Rev. Lett. 57, 1696 (1986). DOI: 10.1103/PhysRevLett.57.1696; 55

[62] Zoller, P. and Marte, M. and Walls, D. F. *Quantum jumps in atomic systems*. Phys. Rev. A 35, 198 (1987). DOI: 10.1103/PhysRevA.35.198; 55

[63] Cook, Richard J. and Kimble, H. J. *Possibility of Direct Observation of Quantum Jumps*. Phys. Rev. Lett. 54, 1023 (1985). DOI: 10.1103/PhysRevLett.54.1023; 55

[64] M. F. Santos and A. R. R. Carvalho. *Observing different quantum trajectories in cavity QED*. EPL 94 64003 (2011). DOI: 10.1209/0295-5075/94/64003; 64

[65] Santos, M. F. and Terra Cunha, M. and Chaves, R. and Carvalho, A. R. R. *Quantum Computing with Incoherent Resources and Quantum Jumps*. Phys. Rev. Lett. 108, 170501 (2012). DOI: 10.1103/PhysRevLett.108.170501; 66

[66] Carvalho, A. R. R. and Santos, M. F. *Distant entanglement protected through artificially increased local temperature*. New J. Phys. 13 013010 (2011). DOI: $10.1088/1367-2630/13/1/013010$; 66

[67] V. Gorini, A. Kossakowski, and E.C. Sudarsahan. *Completely positive semigroups of n-level systems*. J. Math. Phys., 17:821 (1976); 68

[68] G. Lindblad. *On the generators of quantum dynamical semigroups*. Commun. Math. Phys., 119:48 (1976); 68

[69] F. Nicacio and R. N. P. Maia. *Gauge Quantum Thermodynamics of time-local non-Markovian evolutions*, Phys. Rev. A 108, 022209 (2023). DOI: 10.1103/PhysRevA.108.022209; 71

[70] R. Rubboli and M. Tomamichel. *Fundamental Limits on Correlated Catalytic State Transformations*. Phys. Rev. Lett. 129, 120506 (2022); 1, 80

[71] V. Narasimhachar and G. Gour. *Resource Theory under Conditioned Thermal Operations*. Phys. Rev. A 95, 012313 (2017); 1, 80

[72] A. Martin Alhambra. *Non-Equilibrium Fluctuations and Athermality as Quantum Resources*. Doctoral, UCL (University College London), 2017; 1, 80

[73] M. Horodecki and J. Oppenheim. *Quantumness in the Context of Resource Theories*. Int. J. Mod. Phys. B 27, 1345019 (2013); 80

[74] G. Gour. *Role of Quantum Coherence in Thermodynamics*. PRX Quantum 3, 040323 (2022); 80

[75] B. de L. Bernardo. *Unraveling the Role of Coherence in the First Law of Quantum Thermodynamics*. Phys. Rev. E 102, 062152 (2020); 80

[76] Q. A. Turchette, C. J. Hood, W. Lange, H. Mabuchi, and H. J. Kimble. *Measurement of Conditional Phase Shifts for Quantum Logic*. Phys. Rev. Lett. 75, 4710 (1995); 80

[77] Q. A. Turchette, R. J. Thompson, and H. J. Kimble. *One-Dimensional Atoms*. Applied Physics B-Lasers and Optics 60, S1 (1995); 80

[78] A. Auffeves-Garnier, C. Simon, J.-M. Gerard, and J.-P. Poizat. *Giant Optical Nonlinearity Induced by a Single Two-Level System Interacting with a Cavity in the Purcell Regime*. Phys. Rev. A 75, 053823 (2007); 80

[79] O. Astafiev, A. M. Zagoskin, A. A. Abdumalikov, Y. A. Pashkin, T. Yamamoto, K. Inomata, Y. Nakamura, and J. S. Tsai. *Resonance Fluorescence of a Single Artificial Atom*. Science 327, 840 (2010); 80

[80] L. Leandro, J. Hastrup, R. Reznik, G. Cirlin, and N. Akopian. *Resonant Excitation of Nanowire Quantum Dots*. Npj Quantum Inf 6, 1 (2020); 80

[81] J. P. Hadden et al. *Integrated Waveguides and Deterministically Positioned Nitrogen Vacancy Centers in Diamond Created by Femtosecond Laser Writing*. Opt. Lett., OL 43, 3586 (2018); 80

[82] Auffèves, Alexia. *Quantum Technologies Need a Quantum Energy Initiative*. PRX Quantum 3, 020101 (2022). DOI: 10.1103/PRXQuantum.3.020101; 81

[83] J. J. Sanchez-Mondragon and J. C. Garcia-Melgarejo. *Cavity Quantum Electrodynamics on a Cross-Cavity* in Latin America Optics and Photonics Conference, (Optica Publishing Group, 2016), paper LTh2B.6; 81

[84] Brekenfeld, M., Niemietz, D., Christesen, J.D. et al. *A quantum network node with crossed optical fibre cavities*. Nat. Phys. 16, 647?651 (2020). DOI: 10.1038/s41567-020-0855-3; 81

[85] Andre Heinz, Jan Trautmann, Neven Santic, Annie Jihyun Park, Immanuel Bloch, and Sebastian Blatt. *Crossed optical cavities with large mode diameters*. Opt. Lett. 46, 250 – 253 (2021); 81